Recognition of cross-shore dynamics of longshore bars in upper-shoreface deposits of prograding sandy coastal barriers

Van Den Berg, Jan H.; Martinius, Allard W.

Important note
To cite this publication, please use the final published version (if applicable).
Please check the document version above.

RECOGNITION OF CROSS-SHORE DYNAMICS OF LONGSHORE BARS IN UPPER-SHOREFACE DEPOSITS OF PROGRADING SANDY COASTAL BARRIERS

JAN H. van den BERG[1] and ALLARD W. MARTINIUS[2,3]

[1]*Department of Physical Geography, Faculty of Geosciences, Utrecht University, Princetonlaan 8a, Utrecht 3584 CB, The Netherlands*
[2]*Department of Geosciences and Engineering, Delft University of Technology, Stevinweg 1, Delft 2628 CN, The Netherlands*
[3]*Equinor ASA, Arkitekt Ebbellsvei 10, N-7053 Trondheim, Norway*
e-mail: janrikvdb@outlook.com

Abstract: In the past decades it has become evident that the often cyclic cross-shore migration of longshore bars is significantly influenced by wave climate. This study demonstrates that this cyclic migration, whether landward or seaward, leads to the formation of low-angle seaward-inclined stratification (SIS) spanning the beach and upper shoreface in ground-penetrating radar (GPR) data from prograding sandy coastal barriers including strandplains. Previously documented radargrams of these systems are reinterpreted using this knowledge of cross-shore dynamics of longshore bars. Five distinct wave-climate-related radar architectures are identified.

A notable observation is the prevalence of SIS as the dominant upper-shoreface to beach structure in most radargrams, despite its infrequently described occurrence from outcrop observations. To address this disparity, this paper also focuses on recognizing SIS in outcrop and core data. Compelling evidence of SIS was discovered in a late Messinian coastal barrier parasequence in SE Spain, and the associated sedimentary architecture is described in detail. It is hypothesized that this example holds generic significance, illustrated using core data from Middle Jurassic strata of the Norwegian continental shelf, and suggesting that the sedimentary architectures of numerous other ancient prograding barrier deposits may exhibit variations within a similar SIS framework.

INTRODUCTION

The cross-shore migration of longshore bars on sandy coasts typically displays a cyclic behavior characteristic of a specific wave climate (e.g., Davidson-Arnott 2022). This study aims to establish connections between these behavioral variations and the sedimentary architecture of sandy prograding coastal barriers as revealed in cross-sectional ground-penetrating radar (GPR) data of subrecent coastal barrier deposits (Table 1). In these radargrams, a prominent feature often observed is large-scale seaward-inclined low-angle stratification (SIS), which encompasses the beach and upper shoreface (Fig. 1). A secondary objective is to identify evidence of SIS in ancient deposits of prograding coastal barriers, both in outcrop and in core.

Here, a (coastal) barrier is defined as proposed by Dillenburg and Hesp (2009) as a shore-parallel structure, formed by an accumulation of sand, gravel, shells, and small amounts of organic material due to the action of waves, tides, and winds. This definition has the advantage that it includes strandplains and therefore, when applied to ancient deposits, does not require evidence of backbarrier lagoons or marshes, which may be lacking due to erosion. The upper shoreface is defined according to Hamon-Kerivel et al. (2020) as the zone seaward of the beach (mean low-water line), characterized by significant morphologic variability over seasonal to annual timescales, in contrast to the adjacent lower shoreface. This definition acknowledges the importance of longshore bars and rip channels in the formation of sedimentary structures, as well as the erosional processes shaping the lower boundary of the upper shoreface. Given the steep nature of the beach face in gravelly barriers, which lack well-developed longshore bars

(e.g., Wright and Short 1984; Davidson-Arnott 2022), this analysis focuses specifically on coastal barriers composed of sand, with, at most, some admixture of gravel.

SIS typically exhibits decimeter-spaced surfaces. While these surfaces generally appear smooth, it is not uncommon for individual low-angle surfaces to display irregular undulations and occasional erosion, sometimes even eroding into each other (e.g., Fig. 1). In many publications this stratification is labeled as clinoforms, representing timelines of the progradation of the coastal barrier (Fitzgerald et al. 1992; Smith et al. 1999; Goslin and Clemmensen 2017; Oliver et al. 2017; Van Heteren et al. 2018; Berton et al. 2019; Dougherty et al. 2019) because it resembles the coastal time-averaged equilibrium profile.

A well-documented case is the prograding barrier of Long Beach Peninsula, Washington, USA, located north of the mouth of the Columbia River, along the Pacific coast (Figs. 1, 2; Smith et al. 1999; Jol et al. 2002; Moore et al. 2004). At this location, information of GPR profiles of deposits less than a century old can be compared with morphodynamic data of the current upper shoreface (Cohn and Ruggiero 2016; Ruggiero et al. 2016). In the beach zone the presence of seaward-inclined low-angle surfaces is attributed to the well-known flat erosion profiles created during storms on exposed sandy coasts (e.g., Doeglas 1954; Hayes and Boothroyd 1969; Van den Berg 1977; Dougherty 2014). Notably, Moore et al. (2004) identified annual layering in GPR images of the beach and uppermost upper shoreface of a Long Beach Peninsula cross section, that they attributed to erosion during winter storm periods. However, the series of GPR tests performed by Jol et al. (2002) indicated that the SIS can be followed to much lower levels, down

TABLE 1.—*Coastal-barrier radargrams used in this paper. Bar system: Long Beach Peninsula, Cohn and Ruggiero (2016); Kujukuri, Tamura et al. (2007, 2008). * Bar system assumed based on wave climate. Data of tidal range refer to present-day nearby conditions. SIS Max incl., maximum inclination of SIS in upper shoreface deposits; SIS Th., average SIS bed thickness; KP, kink in seaward-inclined low angle GPR strata at about the transition of shore to upper shoreface; BUS, presence base upper shoreface in radargram; LIS, frequent occurrence of sets of low-angle landward-inclined GPR cross-strata.*

	Source	Location		Coastal Setting (see also Table 2)	Signal Freq. (MHz)	Bar System	Mean Tidal Range (m)	SIS Max incl. (°)	SIS Th. (m)	KP	BUS	LIS
1	Barboza et al. 2009	Pinheira Bay	Brazil	South Atlantic Ocean	A	200	non-permanent*	0.6	3	0.6	no	yes	no
2	Dillenburg et al. 2024	Curumim strandplain	Brazil	South Atlantic Ocean	A	200	non-permanent*	0.3	3	0.3	no	no	no
3	Bristow and Pucillo 2006	Guichen Bay	Australia	Southern Ocean	A	100	non-permanent*	0.4	6	0.5	no	no	no
4	Da Rocha et al. 2017	Lagoa de Ribeira	Brazil	South Atlantic Ocean	A	200	non-permanent*	1.1	4	0.2	no	yes	yes
5	Fruergaard et al. 2015	Fanø	Denmark	North Sea	C	100	permanent	1.5	7	0.3	yes	no	no
6	Hede et al. 2015	Nordby Hede, Samsø	Denmark	Kattegat Sea	C	250	permanent	0.3	5	0.2	yes	no	no
7	Jol et al. 2002	Long Beach Peninsula	USA	Pacific Ocean	B	100	permanent	2.0	3	0.5	yes	no	no
8	Nielsen and Clemmensen 2009	Anholt	Denmark	Kattegat Sea	C	250	permanent	0.4	4	0.5	no	no	yes
9	Oliver et al. 2017	Boydtown Bay	Australia	South Pacific Ocean	A	250	non-permanent*	1.5	4	0.2	no	no	yes
10	Oliver et al. 2017	Wonboyn Bay	Australia	South Pacific Ocean	A	250	non-permanent*	1.0	5	0.2	no	no	yes
11	Rodriguez and Meyer 2006	Morgan Peninsula	USA	Gulf of Mexico	C	100	permanent	0.4	8	0.2	no	no	no
12	Santos et al. 2022	Porto Alegre, Xanri-La beach	Brazil	South Atlantic Ocean	A	250	non-permanent*	0.2	2	0.2	no	yes	yes
13	Tamura et al. 2008	Boso Peninsula, Kujukuri plain	Japan	Pacific Ocean	B	100	permanent	1.2	6	0.4	yes	yes	no
14	Van Heteren et al. 2018	Vogelenzang strandplain	Netherlands	North Sea	C	50	permanent	1.6	4	0.4	no	no	no

to 3–5 m in the upper shoreface. The radar information effectively covers most of the upper shoreface, which in the adjacent coasts contains 1–3 longshore bars with troughs extending to depths between 6.8 meters (Ruggiero et al. 2016) and 8 m (Cohn and Ruggiero 2016). The 1–3° seaward-dipping GPR reflectors in this zone cannot be attributed to erosion surfaces from storm events, as in the beach, simply because measurements over many years indicate that the longshore bars are permanent features that are not washed away during storms (Cohn and Ruggiero 2016; Ruggiero et al. 2016).

It is remarkable that longshore bars are not mentioned in many sedimentological studies focusing on the sedimentary architecture of barrier shorefaces (e.g., Olsen et al. 1999; Rodriguez et al. 2001; Fanget et al. 2014). Some barrier models disregard their existence (Reinson 1984; Oertel and Leatherman 1985; Goslin and Clemmensen 2017), despite their significant role in shaping the upper shoreface through interactions with flow and bedforms. To find the shape of the base of reworking by morphodynamic processes, Schwartz and Birkemeier (2004) and Tamura et al. (2007) considered the erosional depth reached by longshore bar troughs obtained from a series of measurements of coastal profiles from a nearby site. This approach can provide valuable insights into intra-shoreface erosional boundaries, particularly those resulting from rapid sea-level fluctuations (Tamura et al. 2007). However, while these bumpy surfaces of maximum erosion may resemble the equilibrium profile of the upper shoreface to some extent, they are composed of distinct erosional events and therefore cannot account for the continuity of SIS observed in many GPR radargrams.

In the past decades it has become clear that longshore bars along many barrier coastlines exist either as a permanent feature along coasts of marginal seas or lakes (Ruessink and Kroon 1994; Wijnberg and Terwindt 1995; Kuriyama 2002; Aagaard et al. 2010; Aleman et al. 2013; Ruggiero et al. 2016; Yuhi et al. 2016) or as temporal alternations with a non-barred shoreface along oceanic coasts (Shepard 1950; Birkemeier 1984; Kuriyama 2002; Tabajara et al. 2008; Short 2020; Ruiz de Alegría-Arzaburu et al. 2022). In most studies of permanent bars along coastal barriers, the longshore bars exhibit a cyclic behavior of seaward migration. This is known as net offshore migration, first described for the Dutch barrier by Ruessink and Kroon (1994) and Wijnberg (1995) and abbreviated as NOM (e.g., Shand et al. 1999; Aleman et al. 2013). Conversely, along many oceanic coasts where barred and non-barred conditions alternate over periods of months to years, bars tend to show a net landward movement (Shepard 1950; Komar 1967; Short 2020; Ruiz de Alegría-Arzaburu et al. 2022), here abbreviated as NLM. This paper will demonstrate that SIS observed in GPR cross sections of upper-shoreface deposits can convincingly be explained by NOM behavior.

So far, the behavior of longshore bars has been described separately for different wave climates. In this paper, we aim to integrate this knowledge with structures observed in radargrams. To accomplish this, first the available understanding of cross-shore dynamics of longshore bars is briefly summarized. Finally, the paper addresses how SIS and associated structures are possibly expressed in outcrop and core, highlighting the need for establishing diagnostic criteria for interpretation.

CYCLIC CROSS-SHORE MIGRATION OF LONGSHORE BARS AS A CAUSE OF LARGE-SCALE LOW-ANGLE CROSS-STRATIFICATION IN GPR PROFILES

Superimposed on the concave-upward equilibrium profile of a sandy upper shoreface (Bruun 1954; Dean 1990; Hamon-Kervel et al. 2020; Davidson-Arnott 2022), generally a system of a single, non-permanent longshore bar, or a permanent multibar bar system, is found. When morphodynamics are not influenced by sand-supply-limited conditions, the presence and dynamics of these bars in sandy shorefaces of coastal barriers is determined by the wave climate. Three morphodynamic systems can be distinguished:
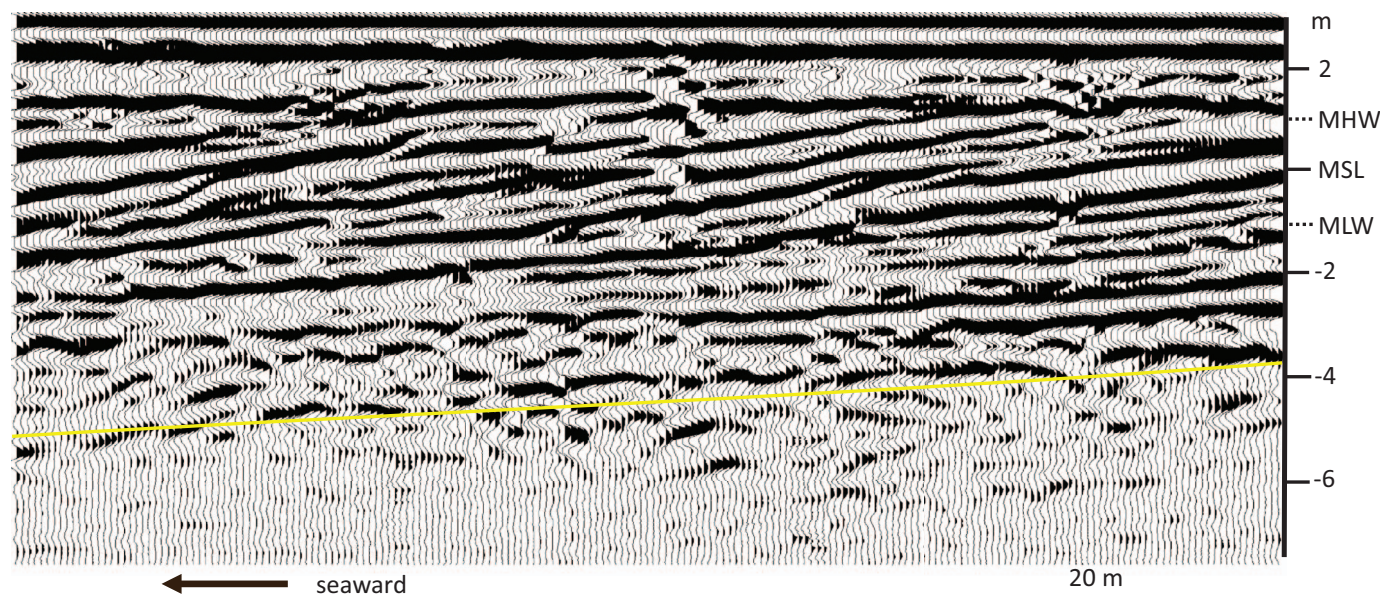
Fig. 1.—Cross-shore radargram (100 MHz) showing offshore inclined low-angle strata in less-than-a-century-old prograding coastal barrier deposits, Long Beach Peninsula, Washington, USA, modified after Jol et al. (2002). Surface elevation obtained from US Topographical Map. For location see Fig. 2. Yellow line shows agreement with scour line deduced from morphodynamic processes in the present-day shoreface (see Fig. 4). MSL, mean sea level; MHW, mean high water; MLW, mean low water.

Non-Permanently Barred Shorefaces

These systems of single, and sometimes double, upper-shoreface bars, characterized by fair-weather long, deep-reaching swell and occasional storm wave conditions, are found along oceanic coasts (e.g., Shepard 1950; Birkemeier 1984; Tabajara et al. 2008; Vidal-Ruiz et al. 2017; Ruiz de Alegría-Arzaburu et al. 2022). The presence of the bars ranges between seldom and of short duration to almost permanent. Their dynamics were first described by Shepard (1950) on the Pacific coast of the USA. During (severe) storm wave events, sand eroded from the beach accumulates in mostly single longshore bars (Shepard 1950; Komar 1967, Silvester 1974). The bar exhibits a NLM behavior and eventually welds on the beach recovering the storm sand loss of the beach and resulting in a temporary non-barred shoreface. During this process, the beach slope increases, or, in terms of the widely used classification scheme of Wright and Short (1984), passes from dissipative to reflective. The occurrence of the opposite process, the destruction of longshore bars during extreme storms, suggested by some researchers (e.g., Bristow and Pucillo 2006; Santos et al. 2022) is unlikely, as it contradicts this mechanism and has never been observed in nature for the sand-rich systems considered here.

Non-Barred Upper Shorefaces

The upper-shoreface bar that is formed in non-permanent systems during storm wave events is built from sand eroded from the beach until, at some point, so much wave energy is dissipated by waves breaking on the bar that beach erosion is retarded. Thus, the bar serves as a natural protection against beach erosion during a severe storm or series of storms, as long as the beach contains enough sand to feed the bar (Silvester 1974; Vousdoukas et al. 2012). If upper-shoreface bars are not formed, the coast will remain unprotected and storm erosion of the beach continues. Therefore the existence of prograding barrier deposits representing non-barred coasts, as suggested in reviews (Galloway and Hobday 1996; Clifton 2006; Tamura 2012; Howell 2020) and outcrop studies (Johnson 1975; Isla et al. 2020a, 2020b) seems incompatible with an assumed presence of storm waves. Isla et al. (2020a) argue that: 1) a very high sand supply rate can make the coastal

profile so steep that bars are not formed and 2) longshore bars, if present, are destroyed during exceptional storm events. However, both processes have never been documented and their occurrence is theoretically unlikely: The supposed steepening is precluded by the very short time frame of adaptation of the beach to upper-shoreface profile to changing conditions, which is in the order of years or even less (Birkemeier 1984; Cowell and Thom 1995; Anthony and Aagaard 2020), following Bruun's equilibrium rule of invariance of this profile relative to the mean sea level (Bruun 1954, 1962). As argued earlier in this paper, severe storms lead to activation of longshore bars instead of their destruction.

Existing facies models of non-barred coastal barrier coasts are based on descriptions by Clifton et al. (1971) and Howard and Reineck (1981). These studies were conducted in a pocket beach and on a location with a narrow shoreface adjacent to a steep offshore ramp. Both sites represent sand-supply-limited conditions, meaning that during severe storms not enough loose sand is available to build a temporary longshore bar. In the case of the south California site (Howard and Reineck 1981), beaches are retained by artificial structures. Most of the sand that is transported alongshore is trapped in the heads of submarine canyons (Griggs et al. 2020) and eventually flushed down canyon by turbidity currents, possibly during breach-failure events as described for a similar canyon along the California coast (Mastbergen and Van den Berg 2003). An indication that supply-limited conditions also apply to the location at the Oregon site comes from a remark that the study area is non-barred "at least within the area of observation" (Clifton et al. 1971, p. 652). Indeed, along the same Oregon coast, in the same wave climate, some kilometers south of the non-barred example, several, possibly non-permanent, barred sites were described by Hunter et al. (1979). They mention that bars are best developed along long, straight, sandy stretches of the Oregon coast. This additional evidence strengthens the hypothesis that the permanent absence of bars in examples studied by Clifton et al. (1971) and Howard and Reineck (1981) is due to sand supply-limited conditions. Theoretically, in a wave climate dominated by long swell and a complete absence of storm waves, bars would never form and a non-barred barrier shoreface might occur. Nevertheless, in his insightful review on the morphodynamics of nearshore bars, Davidson-Arnott (2022, and personal communication 2023) concluded, on the basis of Google Earth images and
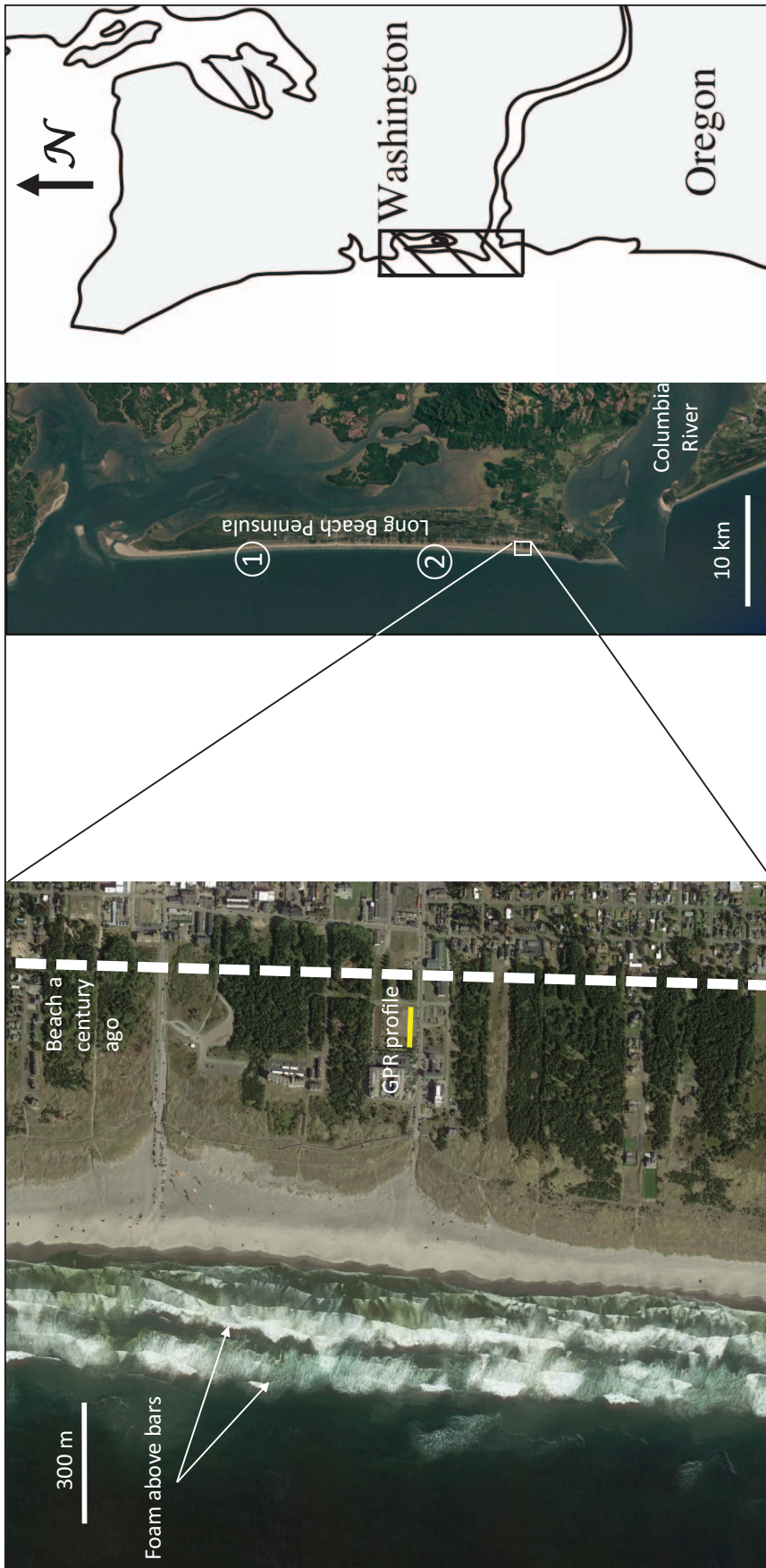
Fig. 2.—Google Earth images with the location of the GPR profile (Fig. 1) and study sites of modern coastal profiles: 1, Cohn and Ruggiero (2016); 2, Ruggiero et al. (2016).
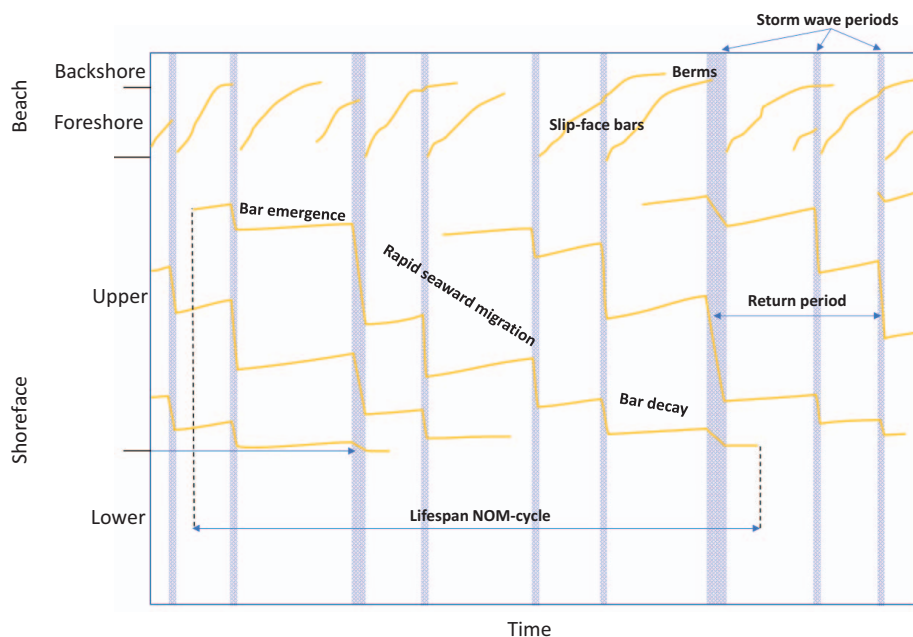
Fig. 3.—Parameters and terms used to define a NOM cycle. Bar-crest migration in the case of a longshore multi-bar system simplified by ignoring the influence of minor storms. Also indicated is the contrasting landward migration of foreshore slip-face bars that may eventually merge on backshore berms and their disappearance during extreme storm events. Based on Grunnet and Hoekstra (2004), Aleman et al. (2017), and short-term process understanding (Van Rijn et al. 2002; Masselink et al. 2006; Walstra et al. 2011; Walstra 2016; Walstra and Ruessink 2017).

his diving experience at many locations in the Caribbean, the presence of non-barred shoreface systems along low-latitude barrier coasts dominated by swell waves and light trade winds, and occasional frequented by storms. For instance, he highlights Manzanilla Beach at the northern tip of the Cocos Bay barrier on the east coast of Trinidad as an illustrative example. Based on soundings, Ibrahim (2005) and Darsan et al. (2012) present different observation from the Caribbean region, indicating that during storms, temporary longshore bars do form on the shoreface, including within Cocos Bay. The apparent contradiction with Davidson-Arnott's non-barred observations may be explained by a quick disappearance of storm-generated bars on these coasts due to rapid landward migration and welding on the beach, caused by strong swell.

So far, in the available literature, conclusive evidence of (almost) permanently non-barred barrier beaches seems to be restricted to the Bay of Aigues Mortes, NW Mediterranean Sea, an area sheltered by a spit (Aleman et al. 2015), where wave refraction produces low steepness waves leading to a dominance of onshore sediment transport, generally impeding the formation of a bar during storm wave events (Davidson-Arnott 2022).

Permanently Barred Upper Shorefaces

In the case of a high storm frequency along oceanic coasts, such as the example north of the mouth of the Columbia River (Fig. 2), time in between storms is insufficient for the removal of upper-shoreface bars (e.g., Wright and Short 1984). Here, and in marginal seas and lakes where long, deep-reaching swell is absent, longshore bars are permanent features and usually more than one bar is present showing a NOM behavior (e.g., Ruessink and Kroon 1994; Wijnberg and Terwindt 1995; Ruggiero et al. 2016). This behavior involves a dynamic interplay characterized by the swift seaward movement of longshore bars during periods of storm waves, juxtaposed with a slower landward migration during extended periods of fair-weather wave conditions. Three distinct phases in the lifecycle of bars are distinguished: their emergence in shallow waters near the beach, subsequent growth and migration seaward, and eventual decline and disappearance at the transition to the lower shoreface (Fig. 3). This process has been described in detail for ocean coasts (Kuriyama 2002; Cohn and Ruggiero 2016; Ruggiero 2016) and sites of marginal seas (Ruessink and Kroon 1994; Wijnberg and Terwindt 1995; Van Rijn et al. 2002; Aagaard et al. 2010; Walstra et al. 2011; Aleman et al. 2013 2015, 2017; Walstra 2016; Yuhi et al. 2016; Walstra and Ruessink 2017; Yuhi

and Uneda 2018). During this process, the inner bar displaces the outer bar, while a new inner bar forms in shallow water. The lifespan of a NOM cycle varies from 1 to 22 years, with migration rates reaching up to 70 m per year (Shand and Bailey 1999; Kuriyama 2002; Aagaard et al. 2010). Notably, along the Gold Coast in southeast Queensland, Australia, a unique bar system exhibits a balance between seaward and landward migration, with non-barred conditions encountered only exceptionally (Ruessink et al. 2009).

Cross-Shore Bar Migration and SIS in a Modern Prograding Coastal Barrier

Interestingly the NOM of shoreface bars was extensively investigated at two locations near the GPR profile depicted in Figure 1, enabling a direct comparison between current cross-shore dynamics of longshore bars and preserved sedimentary structures derived from GPR data. The short-term morphodynamic changes were simulated by Cohn and Ruggiero (2016) for one of these coastal sites using detailed information obtained from two cross-shore profiles at Long Beach Peninsula (Cohn and Ruggiero 2016; Ruggiero 2016) indicated in Figure 2. Figure 4 illustrates the NOM dynamics of the longshore bars in this shoreface. Due to the high frequency of storms at this location, the NOM cycle exhibits a short duration, with a lifespan of 2–6 years. To enhance visualization of the evolution of low-angle erosional surfaces related to the bar–trough system, in Figure 4 a seaward migration rate of up to 40 meters per annum is adopted. This is approximately three times higher than the average seaward accretion rate of the deposits observed in the radargram, as inferred from 19th-century maps (Jol et al. 2002; Fig. 2), and can thus be considered a periodic maximum. It is plausible that along these erosional surfaces, heavy minerals such as magnetite accumulated, forming lag deposits that served as the primary reflectors of the GPR signals (Moore et al. 2004; Smith et al. 1999). The trough landward of the innermost bar starts at a depth of about 2 m below sea level. Unfortunately, the upper part of the shoreface was not included in the profile analysis. Thus, the initiation of the innermost bar is missing. Above this level, the well-known cycle of flat erosional storm beach succeeded by sand recovery through one or more landward migrating ridges or slip-face bars (cf. Masselink et al. 2006) is found. The GPR low-angle strata therefore have at least two origins: in the beach region, the reflectors refer to storm erosion, while in the shoreface the NOM of the longshore bars explains the seaward-dipping GPR
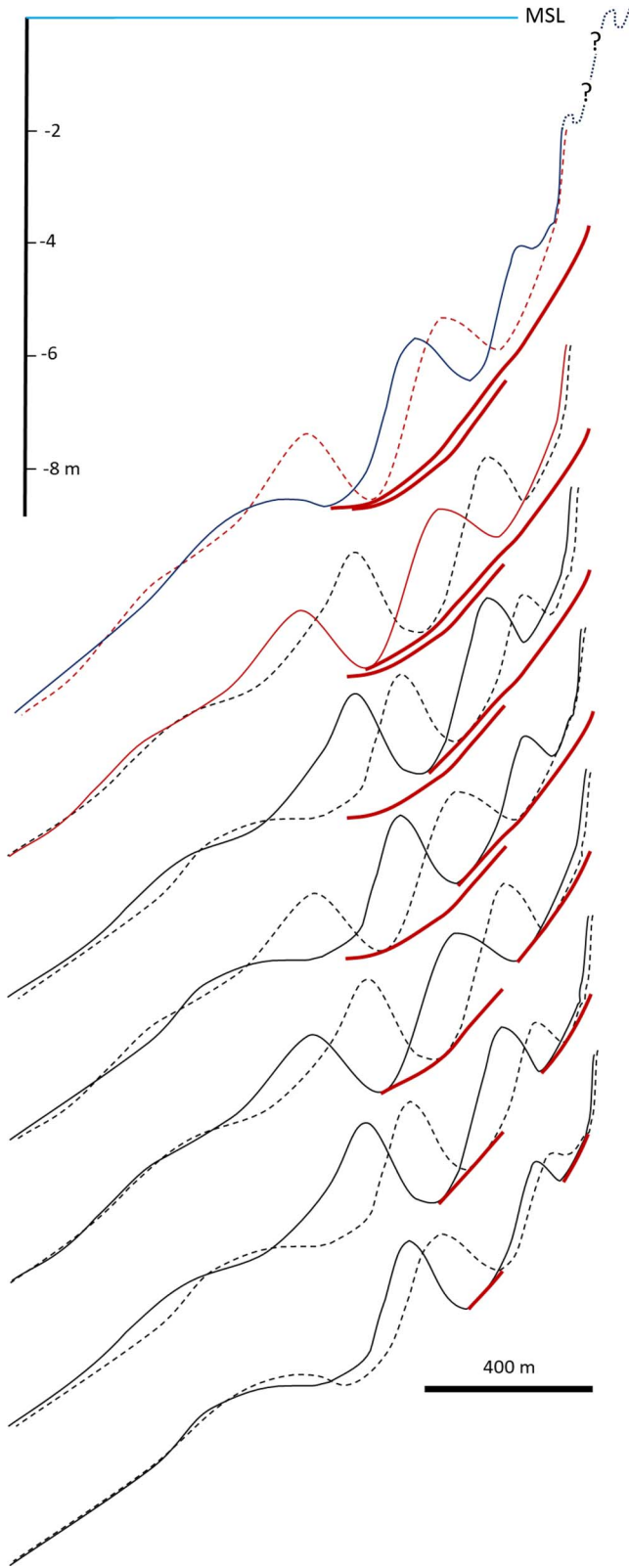
FIG. 4.—Longshore bar configurations in intervals of 3–6 months, depending on wave-energy conditions, at Long Beach Peninsula, based on model simulations (Cohn and Ruggiero 2016). The temporal succession is from base (oldest) to top (youngest). Dashed lines are former configuration, thick red lines are erosion surfaces.
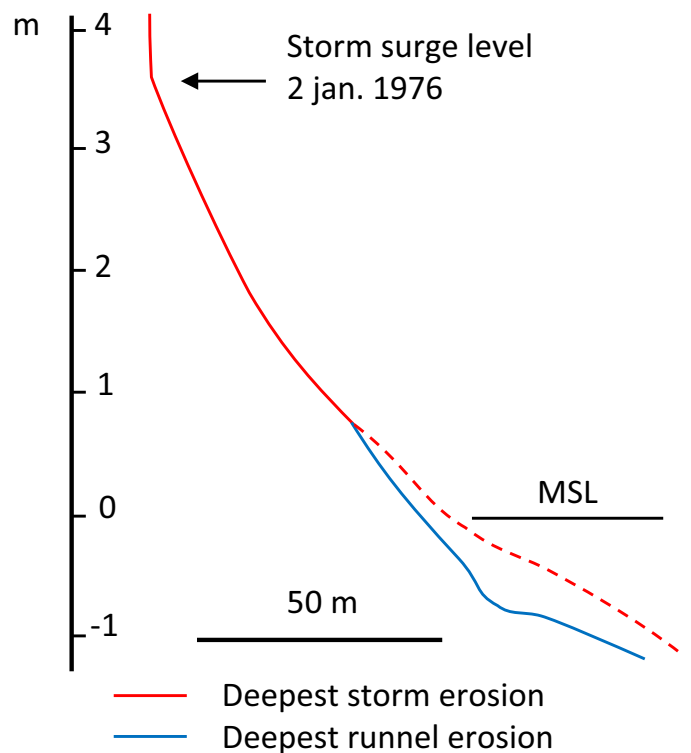
FIG. 5.—Deepest erosional scour of the Zandvoort beach, pole 70, Netherlands, between 2 Jan. 1968 and 6 Jan. 1978. Note that the analysis includes the storm of 2 Jan. 1976, one of the most severe storms of the century. Modified after Van den Berg (1977).

reflectors. An important difference between the two erosion surfaces is that it is synchronous in the beach zone, representing a single storm event, while the offshore-facing low-angle strata in the upper shoreface are diachronous, with a duration equal to the lifespan of a longshore bar, emerging near the beach and ending at the transition to the lower shoreface. In some cases, the picture is further complicated by foreshore runnels that scour deeper than the flat storm profile (Van den Berg 1977). During severe onshore gales due to storm surge, coastal erosion may be concentrated in the dunes and backshore and may be minor or even absent on the lower parts of the beach (Van Rijn 2009). In such cases, the low-angle reflectors of the lower part of the beach represent the scour of a landward-migrating runnel (Fig. 5).

Figure 1 illustrates the longshore trough origin of the SIS in the radargram of Long Beach Peninsula: the concave-upward slope of the bar-trough erosional surface depicted in Figure 4 closely aligns with the GPR strata. The only discrepancy lies in the exclusion of irregularities present in the GPR low-angle strata, which result from irregular depth variations in the bar troughs due to periodic changes in wave conditions not accounted for in the analysis of bar dynamics.

VARIATION IN PROGRADING BARRIER GPR ARCHITECTURE AND PALEOENVIRONMENTAL SIGNIFICANCE

The overall shape of SIS surfaces depicted in the publications listed in Table 1 is concave-upward to sigmoidal. As the SIS approaches the base of the upper shoreface, its slope gradually decreases, eventually becoming nearly horizontal (Van Heteren et al. 2018; Jol et al. 2002; Moore et al. 2004; Bristow and Pucillo 2006; Rodriguez and Meyer 2006; Hede et al. 2015; Dougherty et al. 2018; Da Rocha et al. 2017; Oliver et al. 2017; Santos et al. 2022). In the case of the Long Beach Peninsula, the GPR reflectors are attenuated as they approach a horizontal slope at a depth of

about 6 meters, indicating that the base of the upper shoreface is not much deeper but lies beyond the range of the radar signal. This is supported by morphodynamic studies conducted at the site closest to the location of the radargram (marked 2 in Fig. 2), where the base of the deepest trough (equivalent to the base of the upper shoreface) was measured at 6.8 meters below mean sea level (MSL). At this depth, the seaward-migrating bar troughs erode into lower-shoreface deposits.

It is worth emphasizing that since the NOM-related low-angle bedding is produced by the migration of longshore-bar troughs it is limited to the upper shoreface. Note that this is often a minor part of the total thickness of the shoreface as defined by lithological change (Reineck and Singh 1973). For instance, in the case of the Long Beach Peninsula, well logs indicate that the base of the shoreface is found at depths ranging from 17 to 25 meters (Smith et al. 1999).

During prolonged fair-weather conditions the longshore bar of a non-permanent bar system may weld onto the beach. This process was documented in detail from a large series of cross-shore profile measurements at the field research facility near Duck, located on a coastal barrier facing the Atlantic Ocean (South Carolina, USA). The trough in front of the bar produces a lag deposit that reaches deeper than the flat beach profile immediately after a severe storm event, despite the large amount of sand being eroded from the beach (Schwartz and Birkemeier 2004). The envelope of the profiles or sweepzone of 155 surveys of a cross-shore profile collected between 1981 and 1984 is presented in Figure 6. Note that this envelope represents a stable coastline. In case of progradation, where series of low beach ridges are formed instead of a steep foredune (Hesp 2011), the backshore part of the curve would have a gentler slope. Therefore, the SIS shape in GPR sections of this barrier would resemble that of barriers with permanently barred shorefaces. This observation is corroborated by all radargrams of

barriers with supposed non-permanent bar systems listed in Table 1. The large-scale low-angle strata of such barriers are also diachronous, except for the backshore. However, unlike barriers with permanently barred shorefaces, the seaward-most part of the SIS is deposited first in coastal barriers of non-permanent longshore-bar systems. It is worth noting that according to the widely used definition of a clinoform as a "frozen" paleo-bathymetric profile (Patruno and Helland-Hansen 2018), the partly diachronous SIS of sandy coastal barriers does not strictly meet this criterion.

GPR Structures Superimposed on SIS

In the upper-shoreface zone of certain GPR sections, located between the SIS, units of relatively short, low-angle strata are observed, exhibiting opposing, landward-directed slopes (Hede et al. 2015; Da Rocha et al. 2017; Oliver et al. 2017; Van Heteren et al. 2018; Santos et al. 2022). These strata are interpreted as representing the landward-facing slope of landward-migrating bars (Hede et al. 2015; Santos et al. 2022). In some radargrams of barriers with non-permanent longshore bar systems—and NLM behavior—they are overwhelmingly present (no. 4, 9, 10, and 12 in Table 1). Figure 7 shows an example of this from one of the barrier systems located in southeastern Australia studied by Oliver et al. (2017). The units with strata that climb and erode SIS in these cases were formed both on the upper shoreface and on the beach. On the shoreface they generally exhibit a somewhat steeper slope. To obtain the properties of a reflector, the landward inclined strata possibly represent erosion lags, as with SIS. Regarding the beach, it is speculated that these lags are formed by smoothing of the steep landward-facing slope of slip-face bars during minor storm events (Van Houwelingen 2008). In the case of the Australian examples (nos. 9 and 10 in Table 1), slip-face bars that emerge after a storm can reach a height of several
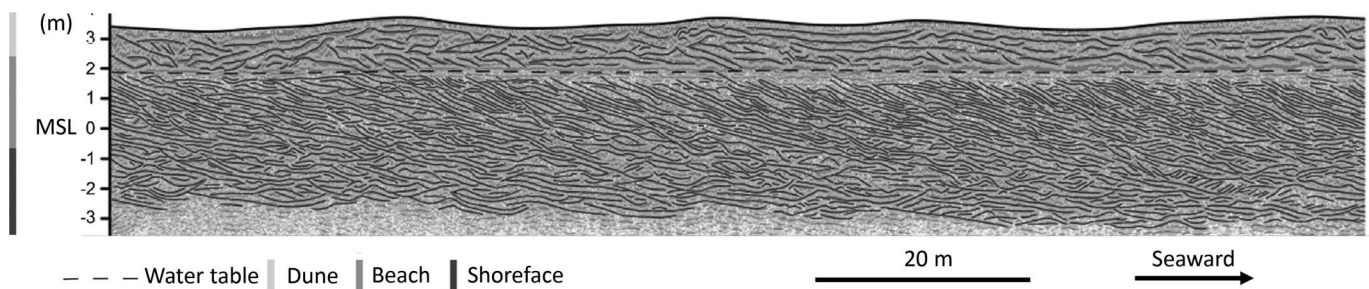
Fɪɢ. 7.—Cross-shore radargram (250 MHz) showing landward-climbing low-angle units downlapping on and sandwiched in between SIS, Boydtown barrier, SE Australia (Fig. 7F in Oliver et al. 2017).
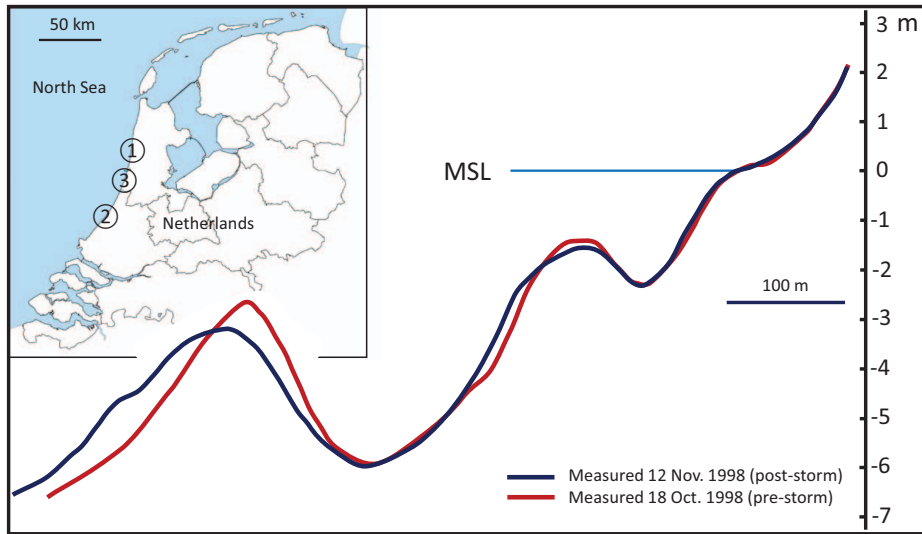
Fig. 8.—Change in average coastal profile at Egmond, Dutch coastal barrier, during a series of three successive storms. The average is based on 10 transects with an alongshore spacing of 100 m. Modified after Van Rijn et al. (2002). 1 Egmond; 2, Noordwijk; 3, Zandvoort.

decimeters (Thom Oliver, personal communication 2023), which aligns with the magnitude recorded in the radargram. With the return of fair-weather wave conditions, the ridges regain their steepness and continue their landward migration. In the upper shoreface, the low-angle landward directed strata have a steeper slope, because the bars retain a steep landward slope during their seaward movement, in both non-permanent (Birkemeier 1984) and permanent (Van Rijn 2002) bar systems. Figure 8 illustrates the change in bar shape after a series of storms for a profile across the Dutch coastal barrier shoreface. Successive low-angle strata are generated by alternating fair-weather and storm-wave conditions. This phenomenon is well documented in studies with high-time-resolution observations of Dutch coastal barrier longshore bars, using video images of foam streaks formed above bars by breaking waves (cf. Fig. 2). An example of such alternations is illustrated in Figure 9. In the radargrams presented by Oliver et al. (2017) and Santos et al. (2022), which frequently display landward-inclined reflectors, relatively short seaward-directed low-angle strata are also observed. Unlike the landward-facing strata,

these seaward-directed strata typically do not form sets of numerous low-angle strata, but instead appear as solitary features or occur in short bundles of 2–3 seaward-directed strata. Santos et al. (2022) interpret these features as the seaward growth or migration of a longshore bar or slip-face bar.

GPR Structures and Longshore Bar Dynamics

Since the introduction of GPR as an aid in detecting sedimentary structures in coastal barriers (Jol et al. 1996), many studies reveal the cross-sectional radar reflector structure of subrecent coastal barrier deposits (Table 1). In the present analysis, this body of research is integrated with the record of the cross-shore dynamics of longshore bars along sandy, stable, or prograding coastal barriers (Table 2). Only radargrams that extend into the deposits of the upper shoreface and exclude complexities introduced by the influence of inlets and spits are considered. For locations in Table 1 typified by non-permanent bar systems, this cannot be determined with certainty because of lack of data. At some of these locations, complete onshore welding and
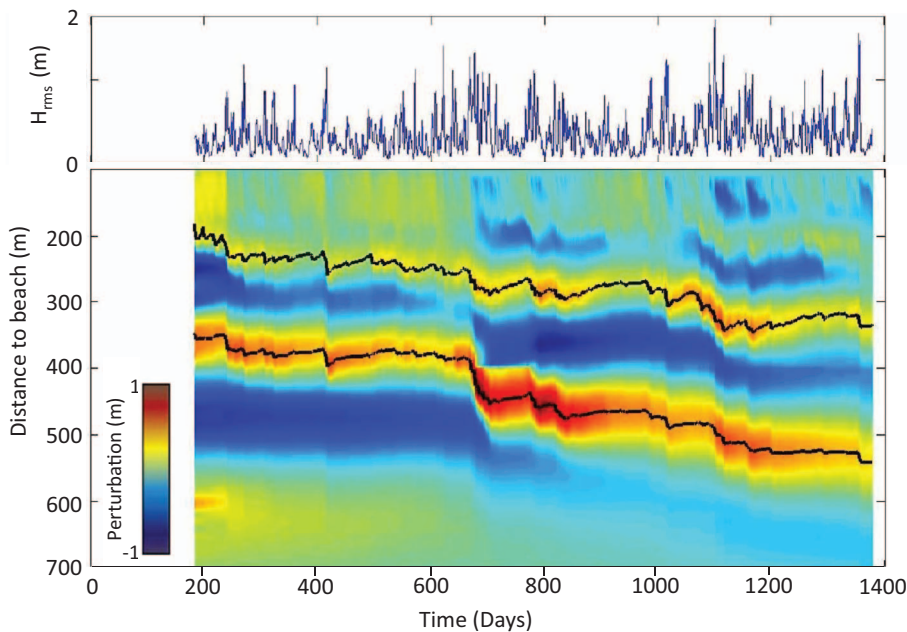
Fig. 9.—Time series of offshore wave height (top) and predicted perturbation with respect to the time-averaged profile of beach pole 80, Noordwijk, Netherlands (location 2 in Fig. 8), for the period 1965 to 1998 (bottom). Black solid lines indicate longshore bar-crest positions. Modified after Walstra et al. (2011).

TABLE 2.—*Basic information of longshore-bar behavior. Data are obtained from locations with at least four cross-shore profiles of a period of more than a decade crossing all longshore bars. Bar migration rates refer to the period of rapid migration as indicated in Figure 3.*

Coastal Setting	nr.	Reference	Location		Number of		Bar Spacing (m)	Deepest Trough		NOM (m/year)	Bar Return Period (Year)
					Surveys	Bars		Depth (m)	Distance to Shore (m)		
A: ocean: occasional storm waves	1	Birkemeier 1984	Duck research facility	NC, USA	Atlantic Ocean	155	0–2	x	5.0	340	x	x
	2	Vidal-Ruiz et al. 2017	Ensenada middle beach	Mexico	Pacific Ocean	28	0–1	x	2.2	240	x	x
	3	Vidal-Ruiz et al. 2017	Ensenada southern beach	Mexico	Pacific Ocean	28	0–1	x	3.5	320	x	x
	4	Ruiz de Alegría-Arzaburu et al. 2022	La Misión beach	Mexico	Pacific Ocean	5	0–2	x	2.5	100	x	x
	5	Shepard 1950	Scripps research facility	CF, USA	Pacific Ocean	13	0–1	x	4.3	80	x	x
	6	Ruessink et al. 2009	Surfers Paradise	Australia	South Pacific Ocean	4	0–2	80–150	4.3	270	x	x
B: ocean: frequent storm waves	7	Ruggiero et al. 2016	Long Beach Peninsula	WA, USA	Pacific Ocean	16	1–3	230–520	6.8	790	220	1–2
	8	Cohn and Ruggiero 2016	Long Beach Peninsula	WA, USA	Pacific Ocean	8	1–3	200–450	10.5	800	270	1.5–3
	9	Kuriyama 2002	Hasaki research facility	Japan	Pacific Ocean	>2000	1–2	50–180	6.8	300	300	1
	10	Aleman et al. 2013, 2015, 2017	Gruissan	France	Gulf of Lions, Mediterranean	11	1–3	90–340	6.5	320	36	11
	11	Aleman et al. 2013, 2015, 2017	Agde	France	Gulf of Lions, Mediterranean	16	1–3	80–300	6.1	210	53	23
	12	Aleman et al. 2013, 2015, 2017	Sète	France	Gulf of Lions, Mediterranean	19	1–3	220–360	6.5	360	69	>16
C: marginal sea/lake fetch > 100–150 km	13	Aleman et al. 2013, 2015, 2017	Maguelone	France	Gulf of Lions, Mediterranean	18	1–2	120–180	5.0	210	19	7–9
	14	Aagaard et al. 2010	Vejers	Denmark	North Sea	5	2–3	300–1000	6.2	450	50	6–10
	15	Ruessink and Kroon 1994; Jarkus data	Terschelling	Netherlands	North Sea	11	2–3	220–600	8.9	900	80	8–11
	16	van Rijn et al. 2002; Jarkus data	Egmond	Netherlands	North Sea	17	2	100–400	6.7	500	50	10–15
	17	Yuhi and Uneda 2018; Yuhi et al. 2016	Chirihama Coast	Japan	Sea of Japan	8	2–3	150–400	6.6	700	120	4
D: marginal sea/lake fetch < 100–150 km	18	Hands 1984	Benona	MI, USA	Lake Michigan	4	4	50–300	5.3	300	x	x
	19	Houser and Greenwood 2005	Burley Beach	Canada	Lake Huron	9	2–3	40–90	4.2	130	x	x
	20	Postacchini et al. 2017	Senigallia	Italy	Adriatic Sea, Mediterranean	5	1–3	20–200	2.5	250	x	x
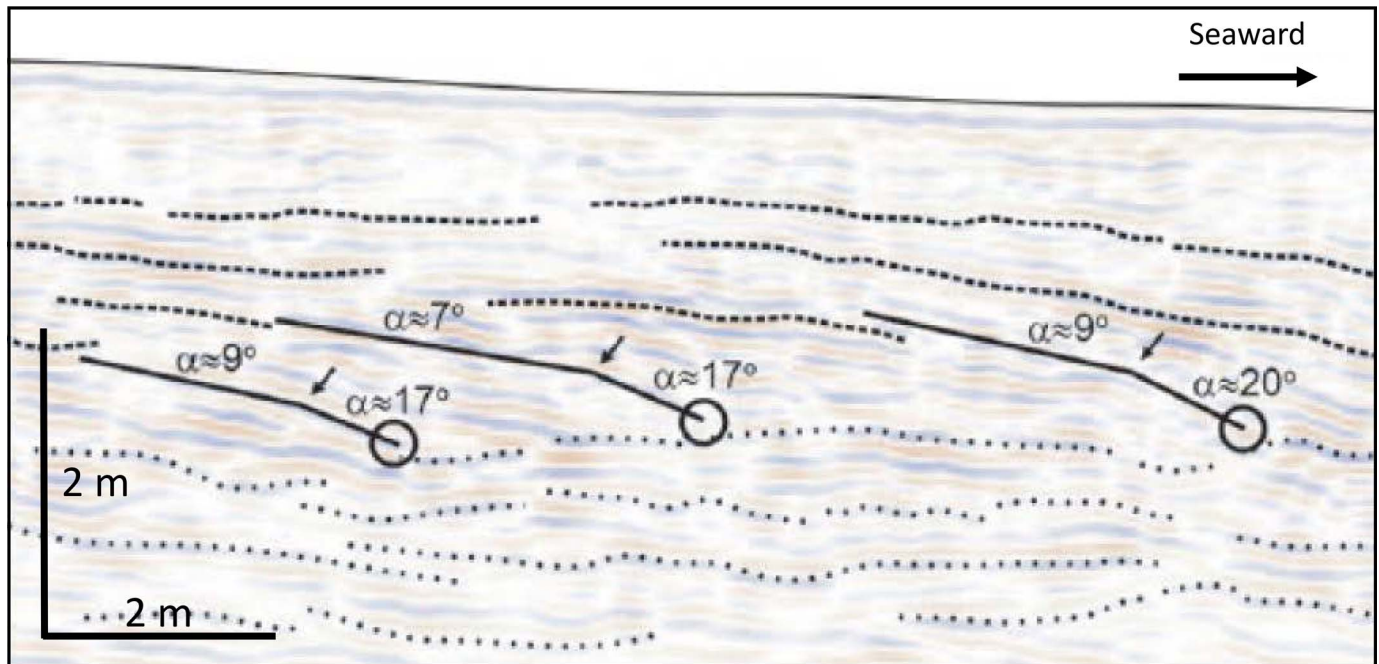
Fig. 10.—Example of GPR reflection data (250 MHz) with interpreted beach-face and upper-shoreface deposits. Raised beach-ridge system, Samsø, Kattegat Sea, Denmark. Note the occurrence of some kinks in the dip that mark the transition of the upper shoreface to the beach (marked by arrows). From Hede et al. (2015). DVR90, Danish Vertical Reference 1990.

disappearance of upper-shoreface bars may rarely be achieved. For instance, near the vicinity of the location of the radargram published by Santos et al. (2022; no. 12 in Table 1), Tabajara et al. (2008) found a permanent presence of one or two longshore bars over a period of eight months, while a cycle of storm erosion and fair-weather recovery affecting a large sediment volume was noted over a much longer timeframe. Therefore, over time the landward transport of sand by swell waves may ultimately lead to the development of a reflective beach face devoid of longshore bars (Short 2020). Thus, while the classification of bar systems as truly non-permanent may not always be conclusive, it is crucial to recognize that in a wave climate dominated by swell waves, there is a prevailing trend towards the landward migration of longshore bars.

The suggestion of Bristow and Pucillo (2006; no. 3 in Table 1) that a transition from the upper shoreface to a muddy substrate on the lower shoreface exists less than two meters below paleo–sea level seems implausible given the high-energy wave conditions that characterize this location. Furthermore, the attenuated reflectors in their radargrams do not exhibit discernible changes that would support the existence of such a transition. It should be noted that reference to estuarine deposits detected in the shallow subsurface south of the position of their radargrams, particularly behind the wave shelter of a protruding Tertiary limestone headland, as outlined by Sprigg (1979), do not substantiate the conclusion of a transition to muddy substrates in the area of interest. Instead of ending in a shallow muddy substrate the radargram shows that SIS continues several meters below this level, as interpreted by Isla et al. (2020a).

The sediment layer sandwiched between two successive low-angle reflectors in GPR sections encompassing the upper shoreface has a maximum duration of deposition equal to a NOM (or NLM) return period (Fig. 3). This duration represents the maximum time frame for net deposition unless the base of the upper stratum eroded previously deposited GPR strata. Given that the formative mechanisms of large-scale low-angle strata in the beach and the shoreface differ, one might anticipate a discontinuity between them. The kink observed in the slope of the strata at the base of the beach, transitioning to a smaller inclination in the upper shoreface, as found in some coastal cross sections

listed in Table 1 (no. 6–8 and 13; Fig. 1) serves as a manifestation of this. A detail of a radargram featuring such kinks is presented in Figure 10. The discontinuity observed in the strata can be caused by: 1) the transition of NOM to NLM behavior in a landward direction, 2) the landward transition to a flat erosional storm beach profile, or 3) the development of a beach step (Bauer and Allen 1995). Beach steps are typically fair-weather features, forming through backwash just below the waterline and generally washed away during storms. However, these steep slopes, which reach heights of 20–40 cm with dip angles near the angle of repose, can be preserved near the low-water level, because erosion of the lower beach during storms is often minimal or absent. Their preservation serves as an indicator of sea level in microtidal regimes (Bardaji et al. 1987; Roep et al. 1998; Nielsen and Clemmensen 2009; Dabrio and Polo 2013; Hede et al. 2015). In the case presented in Figure 10, the strata suggest a beach-step origin for the kink (Hede et al. 2015), buried by swash lamination associated with storm waves.

Variation in GPR architecture Due to Paleowave Climate

So far, the distinction between ancient barrier depositional environments has been limited to low and high wave energy, as proposed by Galloway and Hobday (1996), later refined by Clifton (2006) and extended to a tripartite division by Dashtgard et al. (2021). This classification assumes that in less energetic environments, wave-induced cross-bedding extends less deeply. The fact that the cross-shore behavior of longshore bars is dependent on wave climate raises the question whether this also affects the sedimentary architecture of coastal barriers, potentially allowing for a more nuanced paleoenvironmental distinction. To investigate this idea, the inventory of Table 2 was used.

In non-permanent systems, the migration of bars tends to be quite irregular. Although eventually welding of the bar onto the beach may occur, this process is easily interrupted by recurring storm-wave conditions. For instance, in the case of two locations studied at Ensenada, Mexico (see Table 2, no. 2 and 3), a prolonged period of energetic waves resulted in a six-month delay in the welding process onto the beach. Therefore, statistics regarding NLM behavior

TABLE 3.—*Distinguishing features of prograding coastal-barrier GPR architecture. LIS, frequent occurrence of sets of low-angle landward-inclined strata. Kink, sudden seaward reduction in SIS slope at about the transition of shore to upper shoreface.*

	Coastal Setting		Longshore-Bar System	Behavior	Base Upper Shoreface Depth (m)	GPR Structure	Subrecent GPR Data
A	ocean	occasional storm waves	non-permanent	NLM	2.5–5	SIS + LIS	yes
B	ocean	frequent storm waves	permanent	NOM	6.8–10.5	SIS + kink	yes
C	marginal sea/lake	fetch > 100–150 km	permanent	NOM	5.0–8.9	SIS + kink	yes
D	marginal sea/lake	fetch < 100–150 km	permanent	random	2.5–5.3	chaotic	no
E	all settings	no storm waves	non-barred	X	X	?	no

of non-permanent bar systems, similar to those of NOM in Table 2, do not provide meaningful insights and have not been included. For conditions in lakes and bays with a fetch less than about 100–150 km (i.e., without long and deep-reaching swell) the available data (Table 2, no. 18–20) suggest that cyclic behavior of longshore bars (NOM or NLM) does not occur.

The presence of a kink in the SIS near the low-water mark, as observed in some radargrams in permanent bar systems, seems to signify the transition from NLM to NOM bar behavior. This is supported by the absence of such kinks in radargrams representing non-permanent bar systems, which are characterized by NLM for the entire beach and upper shoreface. Thus, the presence of this kink in GPR cross sections of ancient coastal barrier deposits serves as a criterion for identifying a multi-bar shoreface paleoenvironment with NOM in the upper shoreface. From Table 2, it is evident that longshore bar systems differ in their deepest trough depth (representing the transition from upper to lower shoreface) and, in the case of systems exhibiting NOM behavior, the bar return period, depending on the coastal setting. The absence of NOM in systems with a limited fetch may result in chaotic GPR reflectors in the upper shoreface part of barrier cross sections, potentially illustrating the disorganized behavior of longshore bars in these environments.

The combined information from Table 2 and the understanding of the cross-shore dynamics of longshore bars leads to a tentative differentiation of five types of sandy prograding barrier architecture, as summarized in Table 3. The GPR architecture of prograding barrier deposits along coasts with a limited fetch (Type D in Table 3) remains to be explored. The same holds for permanently non-barred barriers (Type E in Table 3) if such conditions occur. Note that in the latter case the coastal setting of an upper-shoreface deposit can be readily identified by the absence of storm layers in the lower shoreface. Consistent with the findings of Galloway and Hobday (1996), Clifton (2006), and Dashtgard (2021), the depth of transition from upper to lower shoreface increases with wave energy. Oceanic coasts experiencing frequent storm-wave events represent the highest-energy conditions and show the deepest transition to lower shoreface (Type B in Table 3). Oceanic coasts with occasional storms (Type A in Table 3) and water basins with a fetch < 100–150 km (Type D in Table 3) typically have the shallowest upper-to-lower-shoreface boundary. It is worth noting that in small lakes with a fetch on the order of 10 km and less, the troughs of the longshore bars extend even less deeply and the base of the upper shoreface is found at less than 2 meters below lake level (Prieto 1995; Eliot et al. 2006; Nordstrom and Jackson 2012; Ton et al. 2023). Knowledge of their existence and dynamics in coastal barriers, however, is insufficient to incorporate these as a separate class in Table 3. The proposed subdivision in Table 3 serves as a nuanced and extended variant of the models of low- and high-energy barrier facies originally proposed by Galloway and Hobday (1996).

Application of GPR in ancient rocks is hindered by the limited penetration of the required high-frequency electromagnetic signal. The method can only effectively examine deposits that are near a relatively horizontal ground surface. For such conditions GPR imaging technology can provide very good agreement with bedding structures seen in outcrop across a wide range of sedimentological conditions (Akinpelu 2010; Magalhães et al. 2017). One additional advantage of GPR is its capability to enable 3D studies, particularly when an accessible flat operational surface is available

(cf. Coll et al. 2013). However, despite these capabilities, Akinpelu (2010) noted a strong bias towards Quaternary deposits in the application of GPR, a trend that has persisted over the past decades. To date, there has been no reported application of this method to ancient upper-shoreface deposits in outcrop.

RECOGNITION OF BARRIER LOW-ANGLE GPR REFLECTORS IN OUTCROP

This section begins with comparisons between radargrams and outcrop structures, followed by a discussion of potential SIS evidence found in published work. Subsequently, new evidence of SIS from a Miocene coastal barrier deposit in SE Spain is presented.

Dougherty and Nichol (2007) compared structures of beach and eolian dune deposits in a Pleistocene outcrop and a 200 MHz radargram collected close to the outcrop. Good similarity was found for the beach deposits, where up to several-mm-thick laminae of heavy-mineral concentrations are present between sets and strata. However, in the eolian deposits, these heavy-mineral laminae are absent, resulting in a poorer resemblance with only a few faint reflectors visible, despite the presence of detailed structures in the outcrop. Conversely, SIS may be more clearly delineated in GPR images due to their ability to capture subsurface differences in lithology and porosity, which may not be as discernible in outcrop settings (Jol et al. 1996; Akinpelu 2010). Moreover, given its large-scale nature, identifying SIS visually necessitates well-exposed cross sections transverse to the paleocoastline, covering the entire upper shoreface over extensive lengths, conditions that do not occur commonly.

SIS Mentioned in Ancient Upper-Shoreface Deposits

In fact, SIS in upper-shoreface deposits has gone almost unnoticed in outcrop studies, partly due to the paucity of published detailed cross-shore architectural profiles. Consequently, criteria identifying SIS based on recent or sub-recent and outcrop studies are not documented in the literature. Only a few examples exist where the presence of individual large-scale seaward-inclined low-angle strata in shoreface deposits is mentioned. One such instance is documented by Hampson (2000), who identified some of these strata encompassing a 6-meter-thick deposit of a barrier parasequence from the Upper Cretaceous exposed in the Book Cliffs, Utah, USA. These low-angle discontinuities in the upper shoreface "cannot be traced farther paleoseaward." This observation aligns with the understanding that bar-migration-related SIS is confined to the upper shoreface. Given the paleocoastal location of the Western Interior Seaway, it is plausible that SIS originated from NOM behavior of bars in a multibar system with a fetch greater than 100–150 km and maximum bar-trough depths exceeding 5 meters (setting C in Table 3), consistent with the upper-shoreface thickness of the Book Cliffs exposure.

Isla et al. (2020a) described SIS in sandstones of a supposed coastal barrier from the late Valanginian and early Hauterivian in the Neuquén Basin, a large depositional system in the mid-west of Argentina. They interpreted the presence of up to 11° surfaces as evidence of a non-barred shoreface. However, the identification of hummocky cross-stratified sandstone beds in the lower-shoreface, commonly associated with storm events (e.g., Clifton 2006), challenges the interpretation of a non-barred environment, as

F<small>IG</small>. 11.—Google Earth image of location of the outcrops in the Sorbas canyon discussed in this paper. BS, Beach steps studied by Dabrio and Polo (2013).

argued before. Typically, upper-shoreface deposits show multidirectional (swaly/hummocky/normal) cross-bedding and an erosional base cut into finer and more bioturbated beds of the lower-shoreface (Walker and Plint 1992; Galloway and Hobday 1996; Clifton 2006; Pemberton et al. 2012). In contrast, the upper-shoreface deposits discussed by Isla et al. (2020a) show a dominance of unidirectional seaward cross-bedding, that pass gradually into lower-shoreface deposits (Isla et al. 2020a, 2020b), suggesting rip currents as forming agents. Rip channels can erode below the level of the longshore-bar trough in the non-permanent, single bar system of oceanic coasts with occasional storm waves (Hunter et al. 1979), producing dominant seaward-directed cross-bedding at the base of preserved upper-shoreface deposits (Clifton 1981). Soundings and studies using video remote sensing of multibar systems show that rip flows are concentrated in narrow channels that cut through the innermost longshore bar but expand seaward and hardly affect the height of more seaward-located longshore bars (Van Rijn et al. 2002). This means that seaward-directed cross-bedding generated by rip currents may be restricted to the typical non-permanent single-bar systems of oceanic coasts. However, the channelized geometries of rip channels were not observed in the SIS described by Isla et al. (2020a,

2020b). Isla et al. (2020a, 2022) suggest that their barred examples refer to systems with maximum bar-trough depths of about 2 m below MSL, indicating deposition in a sheltered area with a small paleo-fetch. For such conditions, the possibility of bar destruction during severe storms cannot be excluded, given the limited understanding of bar dynamics in these systems. However, such an interpretation challenges their assumption of a coast exposed to high-energy waves.

SIS in a Miocene Coastal Barrier in SE Spain

One of the first detailed descriptions and explanations of sedimentary structures of prograding coastal barrier parasequences was made by Roep et al. (1979, 1998) based on Miocene rocks in the canyon walls below the town of Sorbas, SE Spain (Fig. 11). These barriers were formed in the Neogene Sorbas Basin, which is part of a series of intramontane basins that formed above the exhumed metamorphic zones of the internal Betics (Clauzon et al. 2015). Three superimposed barrier parasequences formed in a 10–15 km wide embayment of the late Messinian Mediterranean, under conditions of practically no infaunal activity (burrowing) due to raised salinities (Roep et al. 1979). Consistent with non-tidal settings, no channel

deposits were found intersecting the barriers. Thus, the barriers possibly consisted of closed systems with a curved outline and one opening through which the small Messinian Río de Aguas paleoriver must have debouched, instead of a series of small barrier islands, as assumed by Martín et al. (1999). Within the scope of the present analysis, the site was revisited. The middle parasequence (parasequence II in Roep et al. 1998) is the best exposed and can be easily observed from a distance at several locations. The analysis presented here is therefore focused on this parasequence.

It is assumed that raised salinities were the result of evaporation in a marginal basin behind a very shallow and narrow connection with the Mediterranean (Braga et al. 2006). However, the transition of lower- to upper-shoreface deposits, which is located at 6 m below assumed paleosealevel (Roep et al. 1979), and the occurrence of fine gravel in deposits of the lower-shoreface indicate that the barrier of parasequence II was formed in an energetic wave climate (Table 3, Type C). This means that high storm waves could pass the sill without losing a significant amount of energy by dissipation and diffraction. More recently, Clauzon et al. (2015) argue that parasequence II was formed in a wedge-shaped depression formed by subaerial erosion during the peak of the Messinian salinity crisis, which contradicts the presence of a sill. Based on dip directions of swash lamination, Roep et al. (1998) concluded that the coastline trended NNW–SSE.

The shoreface deposits show the multidirectional cross-bedding characteristic of this environment. This cross-bedding is generally organized into one or several sets, delineated by horizontal to low-angle surfaces, which may be accentuated by a lag of very coarse sand, occasionally containing some fine gravel (Figs. 12C, D, 13B). As tides were negligible (Roep et al. 1979), the crossbedding was likely produced by dunes migrating in response to wave-generated currents. In an outcrop normal to the paleoshoreline, at the SE side of Sorbas (Fig. 11), low-angle strata encompassing the upper shoreface can be observed over a distance of 120 m (Fig. 12A). Roep et al. (1998) explained this inclination by synsedimentary folding implying a downward bending of the upper- to lower-shoreface boundary. Re-examination of the outcrop, however, shows that this is not the case. Instead, the lower boundary is straight and shows an overall paleoseaward tectonic dip of 2.5°. The strata are either parallel or slightly inclined paleoseaward relative to this dip, and therefore are interpreted as SIS (Fig. 12B). Note that the average spacing of 0.6 m of the bold lines in Figure 12D, interpreted as SIS, falls in the range of 0.2–0.6 m stratal thickness observed in the radargrams listed in Table 1.

The SIS shows a slightly sigmoidal shape, consistent with most radargrams. In the absence of significant tides, the water level remained relatively stable for extended periods, facilitating the formation of beach steps that can produce steep seaward-directed cross-bedding (Bardaji et al. 1987). Dabrio and Polo (2013) described this cross-bedding and associated swash lamination with concentrated heavy-mineral lamination from a nearby location (see Fig. 11). A similar beach-step structure is evident in the outcrop shown in Figure 12B. In this case of a microtidal sea, the top of the beach-step structure roughly corresponds to the base of the beach, indicating a thickness of approximately 7 m for the upper shoreface at this point. In radargrams, beach steps are manifest as kinks in the SIS. However, unlike sub-recent barriers studied with GPR, ancient barrier deposits usually show only partially preserved or completely eroded beach tops, as in the Sorbas case. Consequently, in radargrams of ancient barriers, a kink in the SIS may rarely be present.

These findings highlight the well-organized sedimentary architecture of the upper-shoreface deposits at the Sorbas site, characterized by cross-bedding organized between SIS. The cross-bedding, which is sometimes swaly, exhibits numerous discontinuity planes, multidirectionality, and a prevalence of short set lengths, indicative of the ever changing flow conditions in this environment (e.g., Walker and Plint 1992; Figs. 12C, D, 13B), which in this case are solely caused by varying wind and wave directions. Longshore-directed cross-bedding is dominant, leading to the frequent occurrence of herringbone cross-stratification in outcrops parallel to the paleoshoreline (Fig. 13B). Vertically, there is no discernible change in the style of cross-bedding throughout the upper shoreface. In outcrops aligned along the

paleoshore, the (sub)horizontal strata representing SIS may be truncated by 10–20 m wide, shallow, channelized erosion surfaces, which are interpreted as rip channels (Fig. 13A).

The simple sedimentary architecture observed at the Sorbas site likely results from the cyclic behavior of longshore bars, particularly NOM in this case. Given the prevalence of SIS in most radargrams, it is plausible that the sedimentary architecture of other ancient deposits of prograding barriers show variations of a similar SIS framework. Exceptions to this general trend may arise in barrier deposits formed: 1) in seas or lakes with limited fetch, where cyclic behavior of longshore bars does not occur and 2) in permanently non-barred systems, as the absence of longshore bars in such systems, if they exist, impedes the generation of bar-trough-related SIS.

EXPRESSION OF SIS AND ASSOCIATED STRUCTURES IN CORE

The core repository of the Middle Jurassic stratigraphic record (covering approximately 11 Myr) on the Norwegian Continental Shelf (NCS; Table 4) has been consulted to investigate if and how SIS and associated structures in the upper shoreface are preserved and expressed. To accurately identify SIS in a core dataset, some upfront considerations are necessary regarding three aspects of features that have the potential to enable its identification. Individually, these aspects are not unique to upper-shoreface deposits, and they need to be considered collectively. They include: 1) the potential of the upper-shoreface facies belt on a regressive coastline to become preserved in the subsurface, 2) lithofacies characteristics of upper shoreface including the unambiguous presence of discontinuity surfaces in the succession, and 3) the presence of heavy-mineral concentrations and/or shell–gravel lags, and their identification on seismic lines, and in gamma-ray and density logs. In addition, the consequences of sampling volumes and data resolution of the observational tools deployed need to be considered.

Upper-shoreface lithofacies in the core examples are typified by upper-fine- to lower-medium-grained homogeneous well-sorted sandstone commonly with darker and lighter laminae. In all cases, the darker laminae are rich in mica, and potentially heavy-mineral segregation may occur as well. Cross-stratification dominates in planar to wedge-shaped sets that often truncate each other at low angles, with minor variations in grain size across the set boundaries; characteristic phenomena of the upper shoreface, such as reactivation surfaces (cf. Olsen et al. 1999; Hampson 2000) and occasional Skolithos and Ophiomorpha burrows (Moslow and Pemberton 1988; Reynolds 1992; Cantalamessa et al. 2005; Mitchell et al. 2006; Schwarz et al. 2018) are present.

In recent environments, the inaccessibility of the upper shoreface coupled with a paucity of long (more than 3 m) vibracores (with the exception of the study by Smith et al. 1999) prevents the physical inspection of SIS facies. This hampers the definition of criteria that can be used to recognize discontinuity surfaces in core that can unambiguously be ascribed to SIS in upper-shoreface lithofacies successions. In the case of the selected and deeply buried NCS examples (Table 4), seismic resolution is insufficient to observe lithology contrasts formed by discrete heterogeneities less than 25 cm thick and embedded in well-sorted and homogeneous upper- to lower-shoreface sandstones more than 15 m thick. Lithology contrasts are insufficient, and consequently these architectural features will go unnoticed, including those formed by heavy-mineral concentrations on SIS surfaces or most carbonate-cemented layers. The gamma-ray (GR) borehole logging tool has a resolution of 25 to 30 cm and reacts only to potassium (K), thorium (Th), and uranium (U) elements that occur in the feldspar series and heavy minerals. In addition, there is always background radiation present. Heavy minerals have densities of 2.9 g cm^{-3} or greater (for example magnetite, ilmenite, zircon, rutile, staurolite, kyanite) and unique settling characteristics. In GPR studies of the upper shoreface, heavy-mineral concentrations (lags) are considered to be the main reflectors of the signals received (Moore et al. 2004; Smith et al. 1999; Frihy et al. 2008). Heavy minerals can occur as concentrations in beds of up to 90 cm thick (Smith et al. 1999) but also as dispersed components in shoreface sediment or in mud layers; the latter, however, generally are not
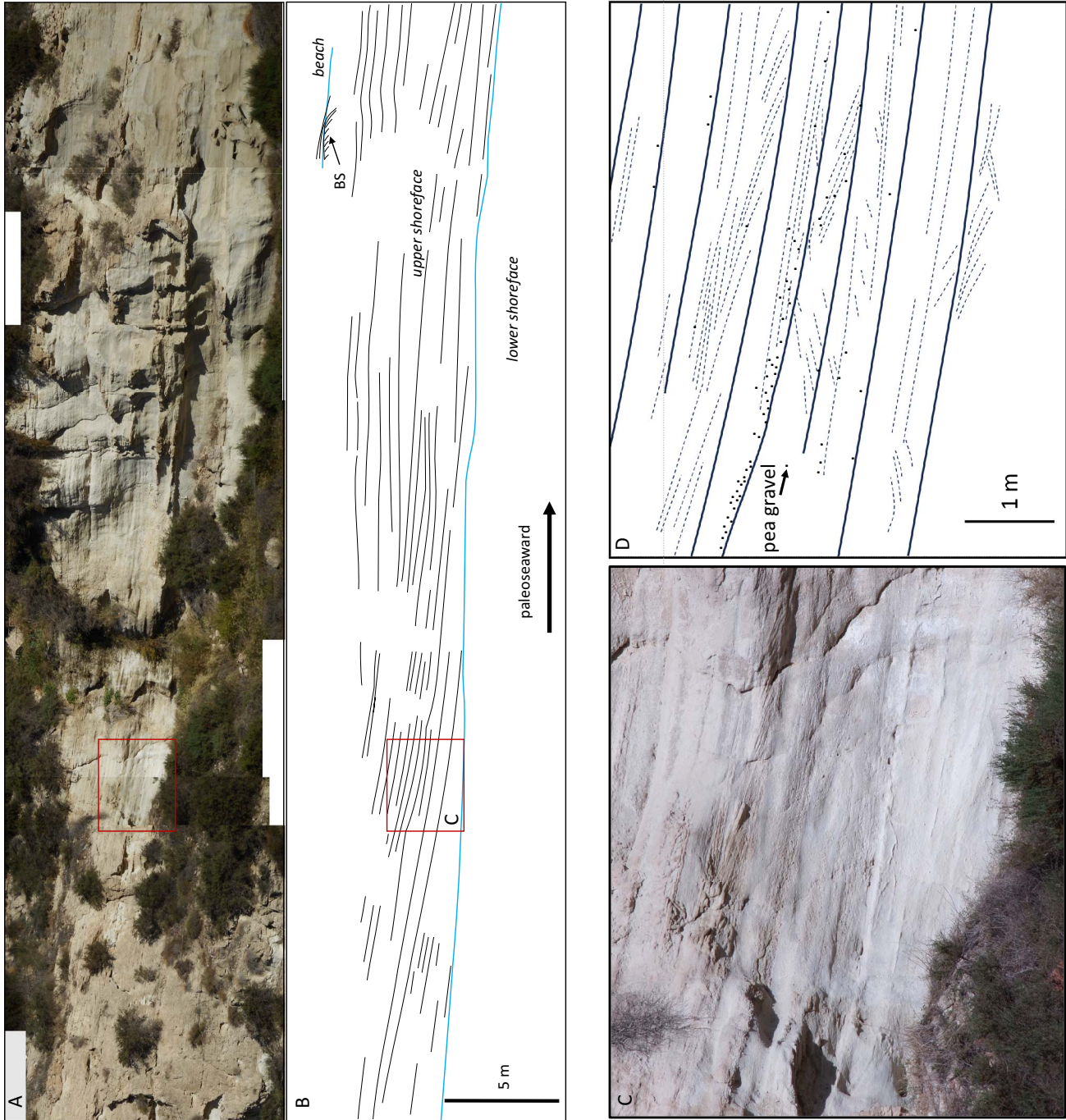
Fig. 12.—SIS in Messinian upper-shoreface deposits, Sorbas. Cross section is perpendicular to oblique to the paleoshoreline (for location and orientation see Fig. 11). **A)** Photomosaic. **B)** Low-angle strata, BS, beach step. C) Detail interpreted in Part D. Solid lines, SIS; dashed lines, multidirectional cross-stratification.
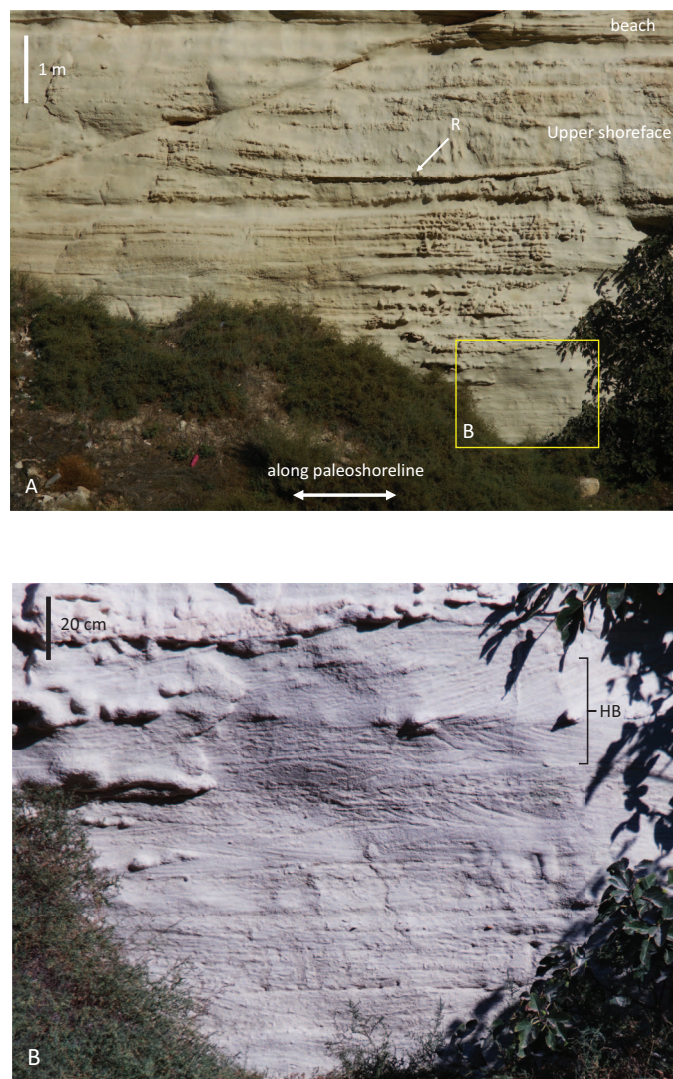
FIG. 13.—Alongshore view of the same upper-shoreface deposits of Figure 12 (for location see Fig. 11). **A)** (Sub)horizontal bedding truncated by a shallow scour, indicated by R. The transition to lower-shoreface is about 1 m below the base of the outcrop. **B)** Detail, showing short multidirectional crossbedding organized between planar surfaces. HB, herringbone cross-stratification.

preserved in upper-shoreface environments. Reynolds (1992), for example, reported an average heavy-mineral content in the total shoreface sand population of the Eocene Meridian Sand Formation (Mississippi, USA) of somewhat less than 2%. In most cases, the heavy-mineral suites are derived from fluvial sources of nearby rivers (Reynolds 1992; Frihy and Komar 1993; Smith et al. 1999). In the studied NCS core, some heavy-mineral concentrations are identified (up to 12%, for example well 34/8-1), but these are thin (a few centimeter thick) and not systematically mapped. In conclusion, in those cases where the GR log possibly records the presence of enhanced gamma-radiation levels, they have been found to be too ambiguous to interpret the presence of heavy-mineral concentrations.

Shell lags in the upper shoreface described in the literature are mostly associated with shoreface ravinement surfaces at temporal scales larger than those represented by a parasequence, but they can also occur at intra-parasequence scale (Fürsich and Aberhan 1990; Kidwell and Bosence 1991). They are identified as coarse transgressive deposits, accumulated as composite, time-averaged concentrations modified by numerous events (i.e., by mixing of skeletal elements of non-contemporaneous populations

or communities, cf. Fürsich and Aberhan 1990). Only within-habitat time-averaged shell lags (assemblages composed of numerous generations from a single community, cf. Kidwell and Bosence 1991) in a regressive setting are valid indicators of SIS. The type of shell concentration leading to shell lags of relevance for this study (cf. Anderson and McBride 1996, their Table 3; see also their Fig. 15) are those formed by numerous storm events causing longshore bar migration and the formation of composite shell concentrations. They form due to winnowing or obrution (smothered by rapid burial), due to which finer terrigenous grain-size fractions may also be removed resulting in relative enrichment of coarser grain-size fractions (such as the inconclusive core example in Fig. 14). Such surfaces may become closely spaced, or even merged, towards the bottom section of a SIS, potentially locally increasing their amalgamated thickness. Characteristics include an erosional base and a gradational top, winnowed, thick, and laterally continuous beds that are often trough cross-stratified, and with poorly organized, imbricated nested fabrics, often with poorly preserved bioclasts. A high sedimentation rate is likely to be the cause of rapid burial and excellent preservation of bioclasts with little or no abrasion. An upper-shoreface shell lag is thus defined here as a concentration of coarse-grained well-preserved shelly material produced by physical sorting and reworking (cf. Anderson and McBride 1996) that is related to the time it took to form a regressive shoreline parasequence. An example of such a deposit of Pleistocene age in the paleo–Tokyo Bay is described by Okazaki and Masuda (1990). These authors identified granule or pumice grains and shell fragments contained in the basal part of longshore bar deposits. Cleveringa (2003) reported thick chaotic shell beds from Holocene upper-shoreface deposits along the Dutch coast, and Van der Valk (1991) found large amounts of bivalve shell material at 5 to 6 m depth in the upper shoreface. Norris (1986) described time-averaged fossil assemblages (coquinas) from upper-shoreface deposits of the Pliocene Purisma Formation (California, USA) interpreted to have been deposited just seaward of the breaker zone in 8–10 m of water. They are composed of amalgamated beds and rounded shell fragments, and may lack bioturbation.

Schwarz et al. (2018) describe preferential concentration of gravel-size and abundant sand-size bioclasts, and terrigenous sand and pebbles present at the base of longshore bar troughs from the Lower Cretaceous Pilmatué Member of the Neuquén Basin (Argentina). These deposits are interpreted as having formed in a storm-dominated regressive shoreface system. Thus, shell lags form in the upper shoreface and can potentially form a detectable surface at the base of a series of offshore-inclined low-angle surfaces associated with longshore bars (SIS). Most mollusk shells are composed of aragonite or high-Mg calcite, an unstable form of carbonate, not likely to leave any body fossils in the rock record after burial and subsequent complex diagenetic history (cf. Worden et al. 2020). It is assumed here that most of the calcite in core originated as bioclastic or micritic debris deposited as lags or scattered throughout the upper-shoreface sands. It then underwent progressive dissolution and reprecipitation during diagenesis, ultimately forming partly or wholly cemented patches or layers up to 1 m thick that can be identified on the density log. Some of the selected examples for this study (Table 4) show cemented intervals in upper-shoreface facies interpreted as originating from shell lags. However, these cases occur in a highly irregular fashion and are uncommon. They are in some cases identified on the density log, but they cannot be used in a conclusive manner. In conclusion, currently SIS cannot be identified with sufficient certainty in core, well logs, or seismic profiles of shoreface successions buried to depths greater than 1 km due to a lack of diagnostic criteria as well as limited tool resolution.

DISCUSSION

The variation in the maximum angle of SIS observed in the available radargrams, ranging from 2° to 8° (Table 1), raises an intriguing question about the underlying factors driving these differences. It is known that the long-term equilibrium slope of the beach upper-shoreface profile tends to decrease with

TABLE 4.—*Selected core intervals from Middle Jurassic formations on the Norwegian Continental Shelf used for this study. Cases not related to barred shorefaces along coastal-barrier coasts (but to other environments where shoreface deposits are identified) were excluded. The combined lower- and upper-shoreface succession had to be at least 20 m thick (with a maximum observed thickness of 72 m) with well-developed lithofacies and exemplified by core material that is of good quality and not fractured to allow reliable inspection and interpretation. Top and base given in core depth (m). The Rannoch, Etive, and Tarbert formations are part of the Brent Group; the Ile Fm is included in the Båt Group. Well information can be accessed through the web pages of the Norwegian Petroleum Directorate, who also preserve the (open source) core material (https://factpages.npd.no/nb-no/wellbore).*

Well	Field	Formation	Top (m)	Base (m)	T (m)	Age
34/7-5	Statfjord Øst	Rannoch Fm	2565	2616	51	Late Toarcian to Bajocian
33/9-4	Statfjord Nord	Rannoch Fm	2836	2879	43	,,
34/7-12	Tordis	Rannoch Fm	2269	2317	48	,,
34/7-13	Vigdis	Rannoch Fm	2523	2563	40	,,
34/7-14	Tordis	Rannoch Fm	2340	2391	51	,,
34/7-16	Vigdis	Rannoch Fm	2443	2490	47	,,
34/7-19	Vigdis	Rannoch Fm	2582	2629	47	,,
34/8-1	Visund	Rannoch Fm	2900	2950	50	,,
34/8-3	Visund	Rannoch Fm	2898	2942	44	,,
34/10-16	Gullfaks Sør	Rannoch Fm	3412	3458	46	,,
34/10-33	Gullfaks Sør	Rannoch Fm	3374	3392	18	,,
34/10-34	Gullfaks Vest	Rannoch Fm	2188	2260	72	,,
34/7-13	Vigdis	Etive Fm	2496	2517	21	Bajocian
34/7-16	Vigdis	Etive Fm	2390	2443	53	,,
6507/7-3	Heidrun	Ile Fm	2385	2408	23	Aalenian
30/9-14	Oseberg Sør	Tarbert Fm	3063	3112	49	Bajocian to Bathonian
30/9-13 S	Oseberg Sør	Tarbert Fm	3024	3084	60	,,

increasing wave energy (e.g., D'Anna et al. 2021). Additionally, this slope is steeper for larger grain sizes (Dean 1987, 1990). The latter may explain the high maximum SIS inclination of 8° of SIS in the Sorbas barrier case, which is developed in medium to coarse sand with some gravel. Information on grain size and wave energy near the radargram locations listed in Table 1, however, is insufficient to investigate this further. The shape of SIS in the shoreface resembles the equilibrium profile. Nonetheless, the troughs between the longshore bars exhibit erosion below this profile. Consequently, SIS exhibits a more pronounced concavity, with steeper contours near the beach zone and gentler slopes transitioning to horizontal closer to the lower-shoreface, as clearly depicted in the radargrams listed in Table 1.

Sets of landward-sloping low-angle strata superimposed on SIS in radargrams possibly represent a non-permanent longshore bar system, characterized by the dominant landward bar migration (Type A in Table 3). However, lack of local information on longshore bar systems in the actual shoreface near the GPR profiles makes it impossible to find out why these bar-edge structures occur in some GPR profiles and not in others. It is worth noting that, in some radargrams, bar flank structures may not have been recognized due to low resolution or signal loss caused by attenuation. Examples of this are GPR sections of the Kujukuri barrier, eastern Japan (Tamura et al. 2008) showing some landward- and seaward-inclined low-angle reflectors. The signal frequency used was only 100 MHz, while in the Australian and Brazilian cases (no. 9, 10, and 12 in Table 1) it was 250 MHz, which may have reduced the detail in the Kujukuri barrier radargram.

Since coastal barrier radargrams generally focus on aspects of barrier progradation, very few are oriented parallel to the barrier. The documented examples show a succession of subhorizontal, slightly undulating strata (Jol et al. 2002; Rodriguez and Meyer 2006; Tamura et al. 2008). This is to be expected because shoreface and beach dynamics are dominated by offshore and onshore movement of bars paralleling the coast. Two radargrams, one from a Japanese coastal barrier facing the Pacific Ocean (Tamura et al. 2008) and the other from the Long Beach Peninsula (Jol et al. 2002), show some counter-oriented discontinuous low-angle strata. Two possible origins are conceivable, either by longshore shift of the 3D morphology of longshore bars or by lateral shift of rip channels. Longshore bars are not completely straight but show alongshore non-uniformities superimposed on the overall straight

base pattern, yielding a three-dimensional morphological system that can vary in time and space between linear, crescentic, and sinuous. The three-dimensionality and variation is greatest for the inner bar (Wright and Short 1984; Van Rijn et al. 2002; Armaroli and Ciavola 2011; Davidson-Arnott 2011, 2022). Crescent-bar morphologies are observed to develop mainly during fair-weather conditions and disappear during storms (Van Enckevort et al. 2004). Another possibility is scour by rip channels. Both features could produce low-angle strata in barrier-parallel GPR sections and can explain their occurrence in the uppermost part of the upper shoreface. The presence of low-angle reflectors about a meter above the transition to the lower-shoreface in the Japanese case, therefore, remains inexplicable. A good example of scour by a rip channel was found in Sorbas parasequence II (Fig. 13A). The base of the channel consists of fine gravel, which could generate a reflector in GPR.

It is important to emphasize that Table 3 is provisional, because it is based on a small database. Further data collection and analysis may lead to alterations or refinements. For example, kinks have been only recorded thus far in radargrams of types B and C coastal settings (Table 1), whereas beach steps, which are one of the causes of kinks, have also been found in outcrops of a Type A setting (De Souza et al. 2012). As mentioned before, the development of beach steps is favored by the absence of tides, and therefore possibly their presence in the geological record points to a micropaleotidal coast.

CONCLUSIONS

Seaward-Inclined, low-angle stratification (SIS) observed in ground-penetration radar (GPR) radargrams of many studies of subrecent coastal barrier deposits, generally spanning the entirety of preserved upper-shoreface to beach deposits of a sandy prograding coastal barrier, has traditionally been interpreted as storm-erosion clinoforms. However, in sand-rich systems, like prograding coastal barriers, this interpretation is unlikely, because longshore bars under such conditions are not destroyed during storm events. In this paper, a reinterpretation of these surfaces is proposed, suggesting that SIS is formed through a combination of synchronous storm-related beach erosion surfaces and diachronous surfaces caused by cross-shore migration of longshore bar troughs. The latter surfaces result from cyclic processes of net landward
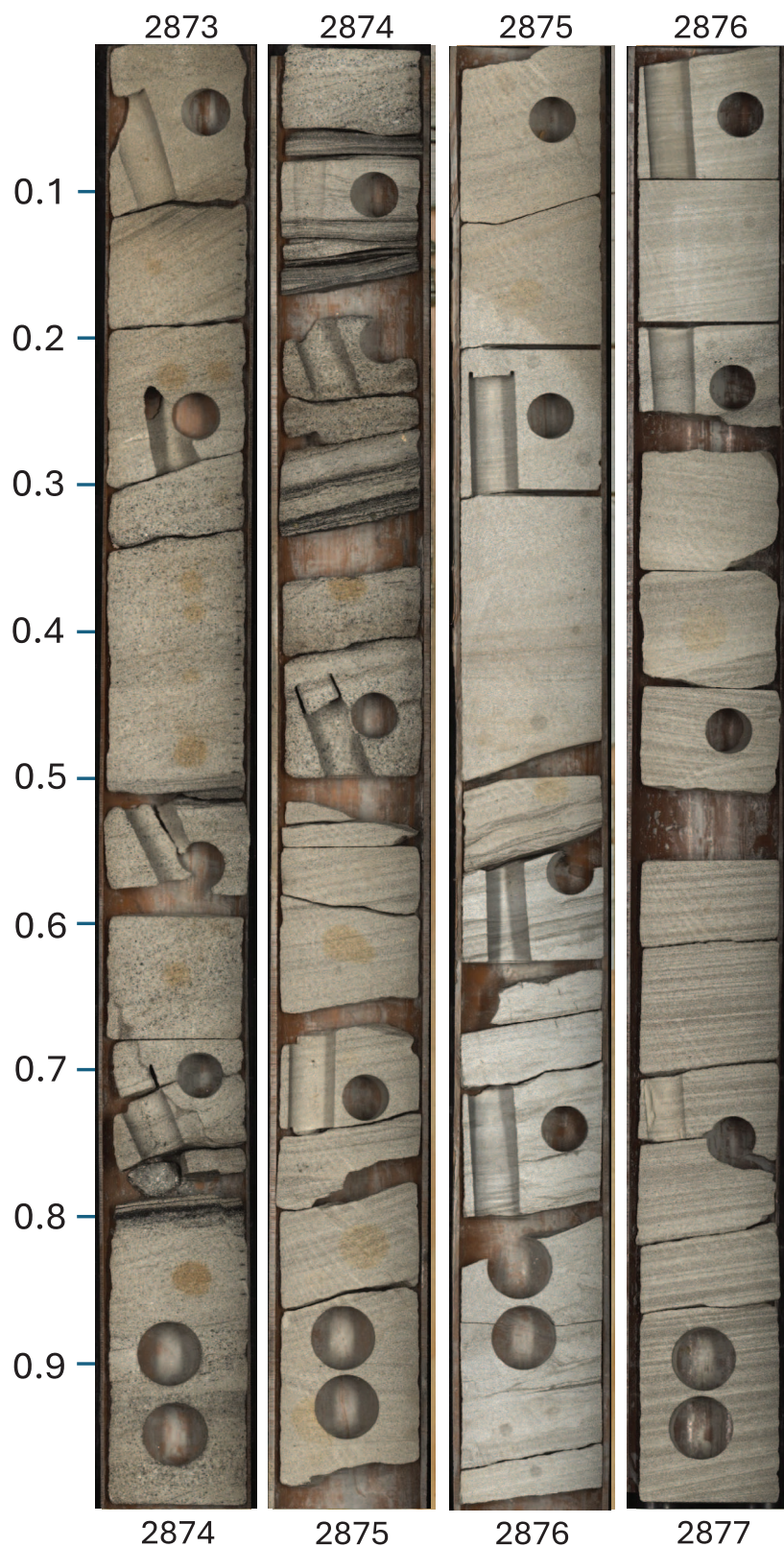
Fig. 14.—Core photo of interval 2873 to 2877 m (core depth) from the upper shoreface of the Rannoch Formation in well 33/9-14 of the Statfjord Nord Field. Note the coarse-grained interval from 2874.5 to 2873.3 m, which is interpreted to be associated with the base of one, and possibly two, superposed, seaward-inclined stratification surfaces.

migration (NLM) or net offshore migration (NOM), determined by the paleowave climate.

In oceanic coastal barriers, SIS can possibly also be formed by the base of rip channels, recognized by a dominance of seaward cross-bedding directions.

Radargrams of coastal barriers with oceanic shores, characterized by long-swell conditions and occasional storm waves, exhibit sets of smaller landward-sloping low-angle strata superimposed on SIS. In marginal seas, such as the North Sea or the Mediterranean, along oceanic coasts with a high frequency of

storms and in very large lakes, longshore bars show a NOM behavior. SIS formed under these conditions may show a kink around the low-water level marking the seaward transition from NLM to NOM. Notably, the depth of the upper-shoreface base varies depending on the wave climate and the frequency of storm occurrences, with oceanic coasts with occasional storms typically showing shallower depths compared to barriers formed along coasts of marginal seas. With limited fetch, the depth of the transition from upper to lower-shoreface is also relatively small. The differences observed suggest a classification of prograding barrier GPR architecture into five types based on wave climate.

Despite its dominant presence in radargrams, SIS has hardly been recognized in outcrop studies due to unfavorable orientation of 2D exposures, limited variation in lithology, and its low-angle nature. Re-evaluation of a Miocene coastal barrier deposit in SE Spain reveals the presence of characteristic multidirectional cross-bedding between regularly spaced low-angle erosion surfaces, containing coarse sand and sometimes some pea gravel. In cross sections normal to the paleoshore the overall shape of this SIS is sigmoidal. Similarity with SIS observed in virtually all published radargrams suggests that most prograding ancient coastal barrier deposits in outcrop likely exhibit a comparable basic sedimentary architecture, except for those formed in seas or lakes with limited fetches or permanently non-barred shorefaces. The latter systems, however, are rare in sandy barriers and are possibly restricted to coarse-grained gravelly barriers, which are not considered here. Further field studies are necessary to validate these conclusions.

Analysis of examples of subsurface shoreface systems using core, well logs, and seismic lines reveal challenges in recognizing SIS due to issues with sampling volumes and tool resolution, and the integration of different data types. Targeted research on exposures and core, using improved criteria for recognition, are essential to translate paleoenvironmental criteria derived from GPR data into the reliable characterization of SIS-related sedimentary structures in outcrop and subcrop.

ACKNOWLEDGMENTS

REFERENCES

AAGAARD, T., KROON, A., GREENWOOD, B., AND HUGHES, M.G., 2010, Observations of offshore bar decay: sediment budgets and the role of lower-shoreface processes: Continental Shelf Research, v. 30, p. 1497–1510.

ALEMAN, N., ROBIN, N., CERTAIN, R., BARUSSEAU, J.-P., AND GERVAIS, M., 2013, Net offshore bar migration variability at a regional scale: inter-site comparison (Languedoc–Roussillon, France): Journal of Coastal Research, v. 165, p. 1715–1720.

ALEMAN, N., ROBIN, N., CERTAIN, R., ANTHONY, E.J., AND BARUSSEAU, J.-P., 2015, Longshore variability of beach states and bar types in a microtidal, storm-influenced, low-energy environment: Geomorphology, v. 241, p. 175–191.

ALEMAN, N., CERTAIN, N.R., ROBIN, N., AND BARUSSEAU, J.-P., 2017, Morphodynamicis of slightly oblique nearshore bars and their relationship with the cycle of net offshore migration: Marine Geology, v. 392, p. 41–52.

AKINPELU, O.C., 2010, Ground penetrating radar imaging of ancient clastic deposits: a tool for three-dimensional outcrop studies [MS Thesis]: University of Toronto, 281 p.

ANDERSON, L.C., AND MCBRIDE, R.A., 1996, Taphonomic and paleoenvironmental evidence of Holocene shell-bed genesis and history on the northeastern Gulf of Mexico shelf: Palaios, v. 11, p. 532–549.

ANTHONY, E.J., AND AAGAARD, T., 2020, The lower-shoreface: morphodynamics and sediment connectivity with the upper shoreface and beach: Earth-Science Reviews, v. 210, no. 103334.

ARMAROLI, C., AND CIAVOLA, P., 2011, Dynamics of a nearshore bar system in the northern Adriatic: a video-based morphological classification: Geomorphology, v. 126, p. 201–216.

BARBOZA, E.G., DILLENBURG, S.R., ROSA, M.L.C.C., TOMAZELLI, L.J., AND HESP, P.A., 2009, Ground penetrating radar profiles of two regressive barriers in southern Brazilian: Journal of Coastal Research, v. 56, p. 579–583.

BARDAJI, T., DABRIO, C.J., GOY, J.L., SOMOZA, L., AND ZAZO, C., 1987, Sedimentologic features related to Pleistocene sea level changes in SE Spain, in Zazo, C., ed., Late Quaternary Sea-Level Changes in Spain: Trabajos sobre el Neogeno–Cuaternario: Museo Nacional de Ciencias Naturales, v. 10, p. 79–93.

BAUER, B.O., AND ALLEN, J.R., 1995, Beach steps: an evolutionary perspective: Marine Geology, v. 123, p. 143–166.

BERTON, F., GUEDES, C.C.F., VESELY, F.F., SOUZA, M.C., ANGULO, R.J., ROSA, M.L., AND BARDOZA, E.G., 2019, Quaternary coastal plains as reservoir analogs: wave-dominated sand-body heterogeneity from outcrop and ground-penetrating radar, central Santos Basin, southeast Brazil: Sedimentary Geology, v. 379, p. 97–113.

BIRKEMEIER, W.A., 1984, Time scales of nearshore profile changes: Houston, Texas, American Society of Civil Engineers, 19th Conference on Coastal Engineering, Proceedings, p. 1507–1521.

BRAGA, J.C., MARTÍN, J.M., RIDING, R., AGUIRE, J., SÁNCHEZ-ALMAZO, I.M., AND DINARÉS-TURELL, J., 2006, Testing models for the Messinian salinity crisis: the Messinian record in Almería, SE Spain: Sedimentary Geology, v. 188–189, p. 131–154.

BRISTOW C.S., AND PUCILLO K., 2006, Quantifying rates of coastal progradation from sediment volume using GPR and OSL: the Holocene fill of Guichen Bay, south-east South Australia: Sedimentology, v. 53, p. 769–788.

BRUUN, P.M., 1954, Coast erosion and the development of beach profiles: U.S. Army Corps of Engineers, Beach Erosion Board, Technical Memoir 44, p. 1–79.

BRUUN, P.M., 1962, Sea-level rise as a cause of beach erosion: American Society of Civil Engineers, Journal of the Waterways and Harbors Division, v. 88, p. 117–130.

CANTALAMESSA, G., DI CELMA, C., AND RAGAINI, L., 2005, Sequence stratigraphy of the Punta Ballena Member of the Jama Formation (Early Pleistocene, Ecuador): insights from integrated sedimentologic, taphonomic and paleoecologic analysis of molluscan shell concentrations: Paleogeography, Paleoclimatology, Paleoecology, v. 216, p. 1–25.

CLAUZON, G., SUC, J.-P., DOCOUTO, D., et al., 2015, New insights on the Sorbas Basin (SE Spain): the onshore reference of the Messinian Salinity Crisis: Marine and Petroleum Geology, v. 66, p. 71–100.

CLEVERINGA, J., 2003, Shoreface stormbeds from Holocene prograded coastal deposits in The Netherlands: Cardiff, 28th Coastal Engineering Conference, Proceedings, p. 2936–2948.

CLIFTON, H.E., 1981, Progradational sequences in Miocene shoreline deposits, southeastern Caliente Range, California: Journal of Sedimentary Petrology, v. 51, p. 165–184.

CLIFTON, H.E., 2006, A reexamination of facies models for clastic shorelines, in Posamentier, H.W., and Walker, R.G., eds., Facies Models Revisited: SEPM, Special Publication 84, p. 293–338.

CLIFTON, H.E., HUNTER, R.E., AND PHILLIPS, R.L., 1971, Depositional structures and processes in the non-barred high-energy nearshore: Journal of Sedimentary Petrology, v. 41, p. 651–670.

COHN, N., AND RUGGIERO, P., 2016, The influence of seasonal to interannual nearshore morphological variability on extreme water levels: modeling wave runup on dissipative beaches: Coastal Engineering, v. 115, p. 79–92.

COLL, M., LÓPEZ-BLANCO, M., QUERALT, P., AND LEDO, J., 2013, Architectural characterization of a delta-front reservoir analogue combining ground penetrating radar and electrical resistivity tomography: Roda Sandstone (Lower Eocene, Graus-Tremp basin, Spain): Geologica Acta, v. 11, p. 27–43.

COWELL, P.J., AND THOM, B.G., 1995, Morphodynamics of coastal evolution, in Carter, R.W.G., and Woodroffe, C.D., eds., Coastal Evolution, Late Quaternary Shoreline Morphodynamics: Cambridge University Press, p. 33–86.

DABRIO, C.J., AND POLO, M.D., 2013, Cyclic coastal sedimentation in Sorbas (Messinian, SE Spain): Geogaceta, v. 54, p. 19–22.

D'ANNA, M., IDIER, D., CASTELLE, B., VITOUSEK, S., AND LE COZANNET, G., 2021, Reinterpreting the Bruun rule in the context of equilibrium shoreline models: Journal of Marine Science and Engineering, v. 9, no. 974.

DA ROCHA, T.B., FERNANDEZAC, G.B., BORGES, G., AND RODRIGUESAD, A., 2017, Registros de erosão e progradação revelados por radar de penetração do solo (GPR) na barreira regressiva pleistocênica do complexo deltaico do Rio Paraíba do Sul (RJ): Quaternary and Environmental Geosciences, v. 08, p. 24–37.

DARSAN, J., RAMNATH, S., AND ALEXIS, C., 2012, Coastal conservation project, Status of beaches and bays in Trinidad (2004–2008): Trinidad and Tobago, Environmental Research Programme, Institute of Marine Affairs, 199 p.

DASHTGARD, S.E., VAUCHER, R., YANG, B., AND DALRYMPLE, R.W., 2021, Wave-dominated to tide-dominated coastal systems: a unifying model for tidal shorefaces and refinement of the coastal environments classification scheme: Geoscience Canada, v. 48, p. 5–22.

DAVIDSON-ARNOTT, R.G.D., 2011, Wave-dominated coasts, in Wolanski, E., and McLusky, D., eds., Treatise on Estuarine and Coastal Science: Elsevier, p. 74–95.

DAVIDSON-ARNOTT, R., 2022, Nearshore bars, in Shroder, J.J.F., ed., Treatise on Geomorphology, Volume 8: Elsevier, p. 247–269.

DE SOUZA, M.C., ANGULO, R.J., ASSINE, M.L., AND CASTRO, D.L., 2012, Sequences of facies at a Holocene storm-dominated regressive barrier at Praia de Leste, southern Brazil: Marine Geology, v. 291, p. 49–62.

DEAN, R.G., 1987, Coastal sediment processes: toward engineering solutions: American Society of Civil Engineers, Proceedings of the Specialty Conference on Coastal Sediments '87, p. 1–24.

DEAN, R.G., 1990, Equilibrium beach profiles: characteristics and applications: Journal of Coastal Research, v. 7, p. 53–87.

DILLENBURG, S.R., AND HESP, P.A., 2009, Coastal barriers: an introduction, *in* Dillenburg, S. R., and Hesp, P.A., eds., Geology and Geomorphology of Holocene Coastal Barriers of Brazil: Springer, p. 1–15.

DILLENBURG, S.R., BARBOZA, E.G., HESP, P.A., ROSA, M.L.C.C., CARON, F., AND GUADAGNIN, F., 2024, The progradational Curumim barrier in southern Brazil: an archive of sea-level changes, and cyclic aeolian activity in the Holocene: Geomorphology, v. 448, no. 109028.

DOEGLAS, D.J., 1954, The origin and destruction of beach ridges: Leidse Geologische Mededelingen, v. 20, p. 34–47.

DOUGHERTY, A.J., 2014, Extracting a record of Holocene storm erosion and deposition preserved in the morphostratigraphy of a prograded coastal barrier: Continental Shelf Research, v. 86, p. 116–131.

DOUGHERTY, A.J., 2018, Prograded coastal barriers provide paleoenvironmental records of storms and sea level during late Quaternary highstands: Journal of Quaternary Science, v. 33, p. 501–517.

DOUGHERTY, A.J., AND NICHOL, S., 2007, 3D stratigraphic models of a composite barrier system, northern New Zealand: Journal of Coastal Research, v. 50, p. 922–926.

DOUGHERTY, A.J., CHOI, J.-H., TURNEY, C.S.M., AND DOSSETO, A., 2019, Technical note: Optimizing the utility of combined GPR, OSL, and Lidar (GOaL) to extract paleoenvironmental records and decipher shoreline evolution: Climate of the Past, v. 15, p. 389–404.

ELIOT, M.J., TRAVERS, A., AND ELIOT, I., 2006, Morphology of a low-energy beach, Como Beach, Western Australia: Journal of Coastal Research, v. 221, p. 63–77.

FANGET, A.-S., BERNÉ, S., JOUET, G., BASSETTI, M.-A., DENNIELOU, B., MAILLET, G.M., AND TONDUT, M., 2014, Impact of relative sea level and rapid climate changes on the architecture and lithofacies of the Holocene Rhone subaqueous delta (Western Mediterranean Sea): Sedimentary Geology, v. 305, p. 35–53.

FITZGERALD, D.M., BALDWIN, C.T., IBRAHIM, N.A., AND HUMPHRIES, S.M., 1992, Sedimentologic and morphologic evolution of a beach-ridge barrier along an indented coast: Buzzards Bay, Massachusetts, *in* Fletcher, C.H., and Wehmiller, J., eds., Quaternary Coasts of the United States: Marine and Lacustrine Systems: SEPM, Special Publication 48, p. 65–75.

FRIHY, O.E., AND KOMAR, P.D., 1993, Long-term shoreline changes and the concentration of heavy minerals in beach sands of the Nile delta, Egypt: Marine Geology, v. 115, p. 253–261.

FRIHY, O.E., HASSAN, M.S., DEABES, E.A., EL MONIEM, A., AND BADR, A., 2008, Seasonal wave changes and the morphodynamic response of the beach–inner shelf of Abu Qir Bay, Mediterranean coast, Egypt: Marine Geology, v. 247, p. 145–158.

FRUERGAARD, M., MØLLER, I., JOHANNESSEN, P.N., NIELSEN, L.H., ANDERSEN, T.J., NIELSEN, L., SANDER, L., AND PEJRUP, M., 2015, Stratigraphy, evolution, and controls of a Holocene transgressive–regressive barrier island under changing sea level: Danish North Sea coast: Journal of Sedimentary Research, v. 85, p. 820–844.

FÜRSICH, F.T., AND ABERHAN, M., 1990, Significance of time-averaging for paleocommunity analysis: Lethaia, v. 23, p. 143–152.

GALLOWAY, W.E., AND HOBDAY, D.K., 1996, Terrigenous Clastic Depositional Systems: Applications to Fossil Fuel and Groundwater Resources: Springer, 489 p.

GOSLIN, J., AND CLEMMENSEN, L.B., 2017, Proxy records of Holocene storm events in coastal barrier systems: storm-wave induced markers: Quaternary Science Reviews, v. 174, p. 80–119.

GRIGGS, G., PATSCH, K., LESTER, C., AND ANDERSON, R., 2020, Groins, sand retention, and the future of Southern California's beaches: Shore & Beach, v. 88, p. 14–36.

GRUNNET, N.M., AND HOEKSTRA, P., 2004, Alongshore variability of the multiple barred coast of Terschelling, The Netherlands: Marine Geology, v. 203, p. 23–41.

HAMON-KERVEL, K., COOPER, A., JACKSON, D., SEDRATI, M., AND GUISADO PINTADO, E., 2020, Shoreface mesoscale morphodynamics: Earth-Science Reviews, v. 209, no. 103830.

HAMPSON, G.J., 2000, Discontinuity surfaces, clinoforms, and facies architecture in a wave-dominated, shoreface–shelf parasequence: Journal of Sedimentary Research, v. 70, p. 325–340.

HAYES, M.O., AND BOOTHROYD, J.C., 1969, Storms as modifying agents in the coastal environment, *in* Hayes, M.O., ed., Coastal Environments: NE Massachusetts: University of Massachusetts, Department of Geology, p. 290–315.

HEDE, M.U., SANDER, L., CLEMMENSEN, L.B., KROON, A., PEJRUP, M., AND NIELSEN, L., 2015, Changes in Holocene relative sea-level and coastal morphology: a study of a raised beach ridge system on Samsø, southwest Scandinavia: The Holocene, v. 25, p. 1402–1414.

HESP, P., 2011, Dune coasts, *in* Wolanski, E., and McLusky, D., eds., Treatise on Estuarine and Coastal Science, Volume 3: Elsevier, p. 193–221.

HOUSER, C., AND GREENWOOD, B., 2005, Profile response of a lacustrine multiple barred nearshore to a sequence of storm events: Geomorphology, v. 69, p. 118–137.

HOWARD, J.D., AND REINECK, H.-E., 1981, Depositional facies of a high energy beach-to-offshore sequence: comparison with low energy sequence: American Association of Petroleum Geologists, Bulletin, v. 65, p. 807–830.

HOWELL, J., 2020, Beaches and coasts, *in* Alderton, D., and Elias, S.A., eds., Encyclopedia of Geology, Second Edition: Elsevier, v. 2, p. 906–918.

HUNTER, R.E., CLIFTON, H.E., AND PHILLIPS, R.L., 1979, Depositional processes, sedimentary structures, and predicted vertical sequences in barred nearshore systems, southern Oregon coast: Journal of Sedimentary Petrology, v. 49, p. 711–728.

IBRAHIM, J.C., 2005, Morphodynamics and surf zone sediment transport for two beaches in Trinidad: response to wet and dry seasons: Journal of Coastal Research, Special Issue: The Sun, Earth and Moon, v. 42, p. 294–302.

ISLA, M.F., CORONEL, M.D., SCHWARZ, E., AND VEIGA, G.D., 2020a, Record of a nonbarred clastic shoreline: Geology, v. 48, p. 338–342.

ISLA, M.F., REMIREZ, M.N., SCHWARZ, E., AND VEIGA, G.D., 2020b, Vertical changes in shoreline morphology at intra-parasequence scale: Latin American: Journal of Sedimentary Basin Analysis, v. 27, p. 85–106.

ISLA, M.F., OLIVO, M.S., ZUAZO, J.I.J., SCHWARZ, E., AND VEIGA, G.D., 2022, Exceptional preservation of a barred shoreline under forced-regressive conditions (Lower Cretaceous, Neuquén Basin, Argentina): Sedimentology, v. 69, p. 891–913.

JOHNSON, H.D., 1975, Tide- and wave-dominated inshore and shoreline sequences from the late Precambrian, Finnmark, North Norway: Sedimentology, v. 22, p. 45–74.

JOL, H.M., SMITH, D.G., AND MEYERS, R., 1996, Digital ground penetrating radar (GPR): a new geophysical tool for coastal barrier research (examples from the Atlantic, Gulf and Pacific Coasts, U.S.A.): Journal of Coastal Research, v. 12, p. 960–968.

JOL, H.M., LAWTON, D.C., AND SMITH, D.G., 2002, Ground penetrating radar: 2D and 3D subsurface imaging of a coastal barrier spit, Long Beach, WA, USA: Geomorphology, v. 53, p. 165–181.

KIDWELL, S.M., AND BOSENCE, D.W.J., 1991, Taphonomy and time-averaging of marine shelly faunas, *in* Allison, P.A., and Briggs, D.E.G., eds., Taphonomy: Releasing the Data Locked in the Fossil Record: Plenum, p. 115–209.

KOMAR, P.M., 1976, Beach processes and sedimentation: Prentice-Hall, 429 p.

KURIYAMA, Y., 2002, Medium-term bar behavior and associated sediment transport at Hasaki, Japan: Journal of Geophysical Research, v. 107, no. 3132.

MAGALHÃES, A., LIMA-FILHO, F., GUADAGNIN, F., SILVA, V., TEIXEIRA, W., SOUZA, A., GABAGLIA, G.R., AND CATUNEANU, O., 2017, Ground Penetrating Radar for Facies Architecture and High-Resolution Stratigraphy: examples from the Mesoproterozoic in the Chapada Diamantina Basin, Brazil: Marine and Petroleum Geology, v. 86, p. 1191–1206.

MARTÍN, J.M., BRAGA, J.C., AND SÁNCHEZ-ALMAZO, I.M., 1999, The Messinian record of the outcropping marginal Alboran basin deposits: significance and implications, *in* Zahn, R., Comas, M.C., and Klaus, A., eds., Proceedings of the Ocean Drilling Program, Scientific Results: College Station, Texas, v. 161, p. 543–551.

MASSELINK, G.A., KROON, G.A., AND DAVIDSON-ARNOTT, R.G.D., 2006, Morphodynamics of intertidal bars in wave-dominated coastal settings: a review: Geomorphology, v. 73, p. 33–49.

MASTBERGEN, D.R., AND VAN DEN BERG, J.H., 2003, Breaching in fine sands and the generation of sustained turbidity currents in submarine canyons: Sedimentology, v. 50, p. 625–637.

MITCHELL, S.E., JAMES, S.A., AND BROWN, I.C., 2006, A late Pleistocene progradational clastic shoreface succession in Jamaica: implications for the preservation potential of the echinoid Leodia: Lethaia, v. 39, p. 321–327.

MOORE, L.J., JOL, H.M., KRUSE, S., VANDERBURGH, S., AND KAMINSKY, G.M., 2004, Annual layers revealed by GPR in the subsurface of a prograding coastal barrier, southwest Washington, USA: Journal of Sedimentary Research, v. 74, p. 690–696.

MOSLOW, T.F., AND PEMBERTON, S.G., 1988, An integrated approach to the sedimentological analysis of some Lower Cretaceous shoreface and delta front sandstone sequences, *in* James, D.P., and Leckie, D.A., eds., Sequences, Stratigraphy, Sedimentology: Surface and Subsurface: Canadian Society of Petroleum Geologists, Memoir 15, p. 373–386.

NIELSEN, L., AND CLEMMENSEN, L.B., 2009, Sea-level markers identified in ground-penetrating radar data collected across a modern beach ridge system in a microtidal regime: Terra Nova, v. 21, p. 474– 479.

NORDSTROM, K.F., AND JACKSON, N.L., 2012, Physical processes and landforms on beaches in short fetch environments in estuaries, small lakes and reservoirs: a review: Earth-Science Reviews, v. 111, p. 232–247.

NORRIS, R.D., 1986, Taphonomic gradients in shelf fossil assemblages: Pliocene Purisima Formation, California: Palaios, v. 1, p. 256–270.

OERTEL, G.F., AND LEATHERMAN, S.P., 1985, Barrier islands: Marine Geology, v. 63, p. 1–18.

OKAZAKI, H., AND MASUDA, F., 1990, Paleodepths and offshore-distances estimated from longshore bar deposits in the Upper Pleistocene Paleo–Tokyo Bay: Sedimentological Society of Japan, Journal, v. 32, p. 117–123.

OLIVER, T.S.N., TAMURA, T., AND HUDSON, J.P., 2017, Integrating millennial and interdecadal shoreline changes: morpho-sedimentary investigation of two prograded barriers in southeastern Australia: Geomorphology, v. 288, p. 129–147.

OLSEN, T.R., MELLERE, D., AND OLSEN, T., 1999, Facies architecture and geometry of landward-stepping shoreface tongues: the Upper Cretaceous Cliff House Sandstone (Mancos Canyon, south-west Colorado): Sedimentology, v. 46, p. 603–625.

PATRUNO, S., AND HELLAND-HANSEN, W., 2018, Clinoforms and clinoform systems: review and dynamic classification scheme for shorelines, subaqueous deltas, shelf edges and continental margins: Earth-Science Reviews, v. 185, p. 202–233.

PEMBERTON, S.G., MACEACHERN, J.A., DASHTGARD, S.E., GINGRAS, M.K., AND ZONNEVELD, J. P., 2012, Shorefaces, *in* Knaust, D., and Bromley, R.G., eds., Trace Fossils as Indicators of Sedimentary Environments: Elsevier, Developments in Sedimentology 64, p. 563–604.

POSTACCHINI, M., SOLDINI, L., LORENZONI, C., AND MANCINELLI, A., 2017, Medium-term dynamics of a middle Adriatic barred beach: Ocean Science, v. 13, p. 719–734.

PRIETO, F.J.G., 1995, Shoreline forms and deposits in Gallocanta Lake (NE Spain): Geomorphology, v. 11, p. 323–335.

REINECK, H.-E., AND SINGH, I.B., 1973, Depositional Sedimentary Environments with Reference to Terrigenous Clastics: Berlin, Springer, 439 p.

REINSON, G.E., 1984, Barrier-island and associated strand-plain systems, *in* Walker, R.G., ed., Facies Models: Geoscience Canada, p. 119–140.

REYNOLDS, W.R., 1992, The heavy-mineral population within the beach sand facies of the Meridian Sand exposed in Mississippi: Gulf Coast Association of Geological Societies, Transactions, v. XLII, p. 633–646.

RODRIGUEZ, A.B., AND MEYER, C.T., 2006, Sea-level variation during the Holocene deduced from the morphologic and stratigraphic evolution of Morgan Peninsula, Alabama, U.S.A.: Journal of Sedimentary Research, v. 76, p. 257–269.

RODRIGUEZ, A.B., FASSELL, M.L., AND ANDERSON, J.B., 2001, Variations in shoreface progradation and ravinement along the Texas coast, Gulf of Mexico: Sedimentology, v. 48, p. 837–853.

ROEP, T.B., BEETS, D.J., DRONKERT, H., AND PAGNIER, H., 1979, A prograding coastal sequence of wave-built structures of Messinian age, Sorbas, Almeria, Spain: Sedimentary Geology, v. 22, p. 135–163.

ROEP, T.B., DABRIO, C.J., FORTUIN, A.R., AND POLO, M.D., 1998, Late highstand patterns of shifting and stepping coastal barriers and washover-fans (late Messinian, Sorbas Basin, SE Spain): Sedimentary Geology, v. 116, p. 27–56.

RUESSINK, B.G., AND KROON, A., 1994 The behavior of a multiple bar system in the nearshore zone of Terschelling, The Netherlands: 1965–1993: Marine Geology, v. 121, p. 187–197.

RUESSINK, B.G., PAPE, L., AND TURNER, I.L., 2009, Daily to interannual cross-shore sandbar migration: observations from a multiple sandbar system: Continental Shelf Research, v. 29, p. 1663–1677.

RUGGIERO, P., KAMINSKY, G.M., GELFENBAUM, G., AND COHN, N., 2016, Morphodynamics of prograding beaches: a synthesis of seasonal- to century-scale observations of the Columbia River littoral cell: Marine Geology, v. 376, p. 51–68.

RUIZ DE ALEGRÍA-ARZABURU, A., VIDAL-RUIZ, J.A., GARCÍA-NAVA, H., AND ROMERO-ARTEAGA, A., 2022, Subaerial and upper-shoreface morphodynamics of a highly-dynamic enclosed beach in NW Baja California: Geomorphology, v. 413, no. 10833.

SANTOS, N.B., LAVINA, E.L.C., PAIM, P.S.G., TATUMIC, S.H., YEEC, M., SANTOS, V.O., AND KERN, H.P., 2022, Relative sea level and wave energy changes recorded in a micro-tidal barrier in southern Brazil: Quaternary Research, v. 110, p. 13–25.

SCHWARTZ, R.K., AND BIRKEMEIER, W.A., 2004, Sedimentology and morphodynamics of a barrier island shoreface related to engineering concerns, Outer Banks, NC, USA: Marine Geology, v. 211, p. 215–255.

SCHWARZ, E., VEIGA, G.D., ÁLVAREZ TRENTINI, G., ISLA, M.F., AND SPALLETTI, L.A., 2018, Expanding the spectrum of shallow-marine, mixed carbonate–siliciclastic systems: processes, facies distribution, and depositional controls of a siliciclastic-dominated example: Sedimentology, v. 65, p. 1558–1589.

SHAND, R.D., AND BAILEY, D.G., 1999, A review of net offshore bar migration with photographic illustration from Wanganui, New Zealand: Journal of Coastal Research, v. 15, p. 365–378.

SHAND, R.D., BAILEY, D.G., AND SHEPHERD, M.J., 1999, An inter-site comparison of net offshore bar migration characteristics and environmental conditions: Journal of Coastal Research, v. 15, p. 750–765.

SHEPARD, F.P., 1950, Longshore bars and longshore troughs. U.S. Army Corps of Engineers, Beach Erosion Board, Technical Memo 15, 32 p.

SHORT, A.D., 2020, Australian Coastal Systems: Beaches, Barriers and Sediment Compartments: Springer, Coastal Research Library, v. 32, 1241 p.

SILVESTER, R., 1974, Coastal Engineering: Elsevier, 338 p.

SMITH, D.G., MEYERS, R.A., AND JOL, H.M., 1999, Sedimentology of an upper-mesotidal (3.7 m) Holocene barrier, Willapa Bay, SW Washington, U.S.A.: Journal of Sedimentary Research, v. 69, p. 1290–1296.

SPRIGG, R.C., 1979, Stranded and submerged sea-beach systems of southeast South Australia and the aeolian desert cycle: Sedimentary Geology, v. 22, p. 53–96.

TABAJARA, L.L.C.A., ALMEIDA, L.E.S.B., AND MARTINS, L.R., 2008, Morfodinâmica bi-tridimensional de praia e zona de surfe intermediária-dissipativa no litoral Norte-RS: Gravel, v. 6, p. 81–97.

TAMURA, T., 2012, Beach ridges and prograded beach deposits as paleoenvironment records: Earth-Science Reviews, v. 114, p. 279–297.

TAMURA, T., NANAYAMA, F., SAITO, Y., MURAKAMI, F., NAKASHIMA, R., AND WATANABE, K., 2007, Intra-shoreface erosion in response to rapid sea-level fall: depositional record of a tectonically uplifted strand plain, Pacific coast of Japan: Sedimentology, v. 52, p. 1149–1162.

TAMURA, T., MURAKAMI, F., AND NANAYAMA, F., 2008, Ground-penetrating radar profiles of Holocene raised-beach deposits in the Kujukuri strand plain, Pacific coast of eastern Japan: Marine Geology, v. 248, p. 11–27.

TON, A.M., VINCENT VUIK, V., AND AARNINKHOF, S.G.J., 2023, Longshore sediment transport by large-scale lake circulations at low-energy, non-tidal beaches: a field and model study: Coastal Engineering, v. 180, no. 104268.

VAN DEN BERG, J.H., 1977, Morphodynamic development and preservation of physical sedimentary structures in two prograding recent ridge and runnel beaches along the Dutch coast: Geologie en Mijnbouw, v. 56, p. 185–202.

VAN DER VALK, L., 1991, Molluscan shell distribution and sediments of the fossil and modern upper shoreface of the coast of Holland (Holocene, W. Netherlands): Contributions to Tertiary and Quaternary Geology, v. 28, p. 13–28.

VAN ENCKEVORT, I.M.J., RUESSINK, B.G., COCO, G., SUZUKI, K., TURNER, I.L., PLANT, N.G., AND HOLMAN, R.A., 2004, Observations of crescentic nearshore sandbars: Journal of Geophysical Research, v. 109, no. C06028.

VAN HETEREN, S., VAN DAM, R.L., CLEVERINGA, J., VAN DER SPEK, J.F., OOST, A., AND STORMS, J.E.A., 2018, Imaging coastal facies in The Netherlands using ground-penetrating radar: Copenhagen, International Association of Sedimentologists, 19th Regional Meeting of Sedimentology, 3 p.

VAN HOUWELINGEN, S.T., MASSELINK, G., AND BULLARD, J.E., 2008, Dynamics of multiple intertidal bars over nondiurnal and lunar tidal cycles, North Lincolnshire, England: Earth Surface Processes and Landforms, v. 33, p. 1473–1490.

VAN RIJN, L.C., RUESSINK, B.G., AND MULDER, J.P.M., 2002, Coast 3D-Egmond: the behavior of a straight sandy coast on the time-scale of storms and seasons: Aqua Publications, Process Knowledge and Guidelines for Coastal Management, 52 p.

VAN RIJN, L.C., 2009, Prediction of dune erosion due to storms: Coastal Engineering, v. 56, p. 441–457.

VIDAL-RUÍZ, J.A., AND RUIZ DE ALEGRÍA-ARZABURU, A., 2017, An annual cycle of sandbar migration on an intermediate mesotidal beach: Ensenada, Mexico, in Aagaard, T., Deigaard, R., and David Fuhrman, D., eds., Proceedings Coastal Dynamics: Helsingør, Denmark, p. 557–585.

VOUSDOUKAS, M.I., ALMEIDA, L.P.M., AND FERREIRA, O., 2012, Beach erosion and recovery during consecutive storms at a steep-sloping, meso-tidal beach: Earth Surface Processes and Landforms, v. 37, p. 583–593.

WALKER, R.G., AND PLINT, A.G., 1992, Wave- and storm-dominated shallow marine systems, in Walker, R.G., and James, N.P., eds., Facies Models: Response to Sea Level Change: Geological Association of Canada, p. 219–238.

WALSTRA, D.J.R., 2016, On the anatomy of nearshore sandbars [MS Thesis]: University of Delft, The Netherlands, 138 p.

WALSTRA, D.J.R., AND RUESSINK, B.G., 2017, Recent insights into inter-annual sandbar dynamics, in Aagaard, T., Deigaard, R., and Fuhrman, D., eds., Proceedings Coastal Dynamics, Helsingør, Denmark, p. 522–533.

WALSTRA, D.J.R., RUESSINK, B.G., AND RANASINGHE, R., 2011, Influence of initialization on inter-annual model predictions, in Wang, P., Rosati, J.D., and Roberts, T.M., eds., Proceedings of Coastal Sediments, v. 1, p. 859–872.

WIJNBERG, K.M., 1995, Morphologic behaviour of a barred coast over a period of decades [MS Thesis]: Utrecht University, 245 p.

WIJNBERG, K.M., AND TERWINDT, J.H.J., 1995, Extracting decadal morphological behaviour from high-resolution, long-term bathymetric surveys along the Holland coast using eigenfunction analysis: Marine Geology, v. 126, p. 301–330.

WORDEN, R.H., MORRALL, G.T., KELLY, S., MCARDLE, P., AND BARSHEP, D.V., 2020, A renewed look at calcite cement in marine-deltaic sandstones: the Brent Reservoir, Heather Field, northern North Sea, UK, in Dowey, P., Osborne, M., and Volk, H., eds., Application of Analytical Techniques to Petroleum Systems: Geological Society of London, Special Publication 484, p. 305–335.

WRIGHT, L.D., AND SHORT, A.D., 1984, Morphodynamic variability of surf zones and beaches: a synthesis: Marine Geology, v. 56, p. 93–118.

YUHI, M., AND OMEDA, S., 2018, Characteristics of systematic migrations of multiple sandbars and related cross-shore sediment transport at Chirihama and adjacent coasts, Japan: Journal of Coastal Research, v. 85, p. 231–235.

YUHI, M., MATSUYAMA, M., AND HAYAKAWA, K., 2016, Sandbar migration and shoreline change on the Chirihama coast, Japan: Journal of Marine Science and Engineering, v. 4, no. 40.